


Transverse Spin Physics with STAR Forward Detectors

Len K. Eun
Penn State University
LANL, Nov. 2010

Transverse Single Spin Asymmetry (A_N)

Transverse single spin asymmetry is measured by the analyzing power, A_N.

$$A_N = \frac{d\sigma^{\uparrow} - d\sigma^{\downarrow}}{d\sigma^{\uparrow} + d\sigma^{\downarrow}}$$ (when measured on the left side of the beam)

$d\sigma^{\uparrow(\downarrow)}$ – differential cross section of π^0 when incoming proton has spin up(down)

π^0 cross section at forward region shows ***left-right asymmetry*** depending on the ***transverse polarization*** of the incoming Proton.

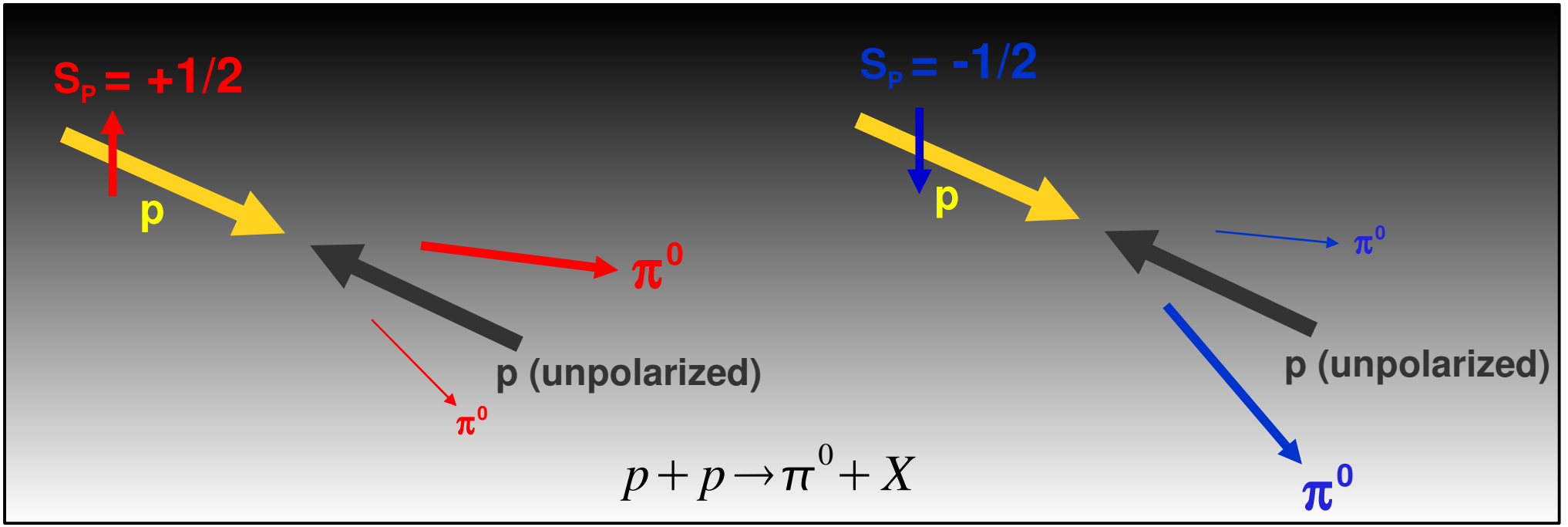

Parton Picture of Scattering

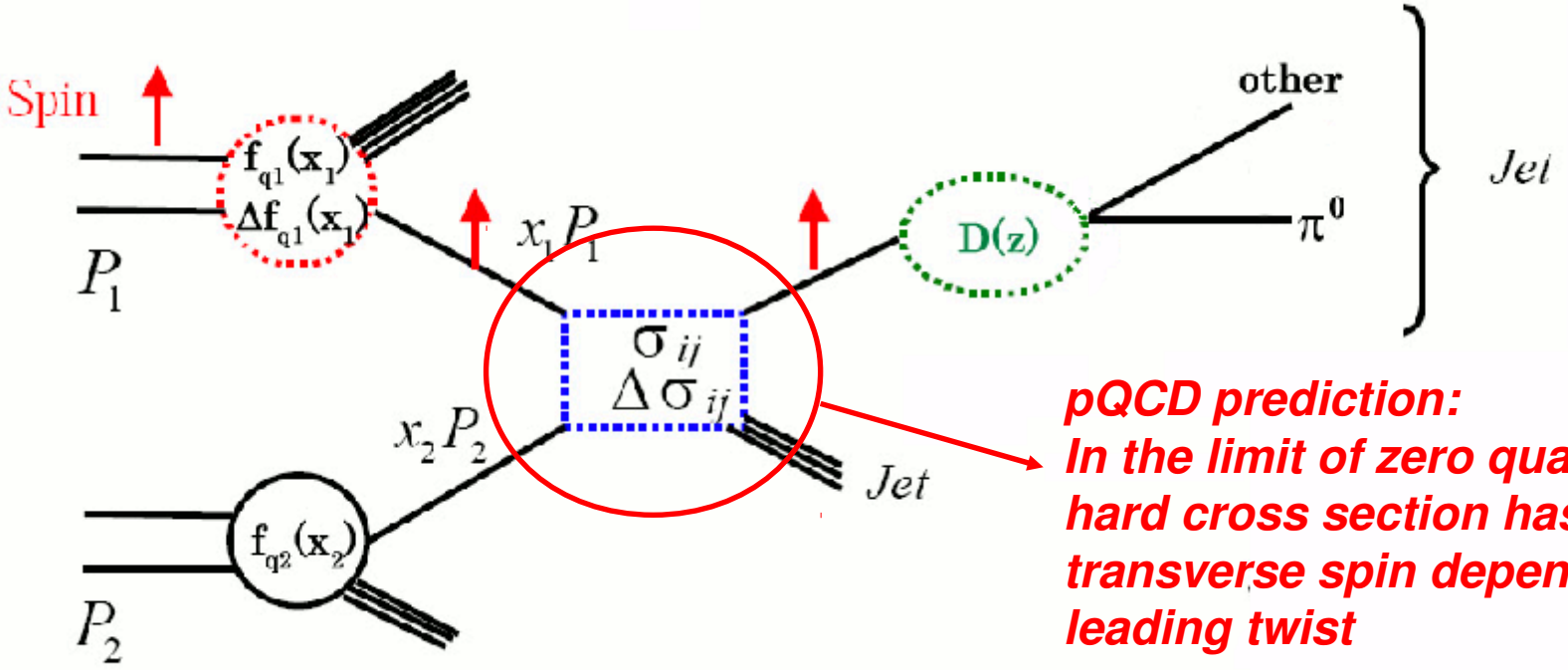

pQCD prediction:
In the limit of zero quark mass, hard cross section has no transverse spin dependence in leading twist

$f_q(x)$: quark Parton Density Function of an unpolarized proton

$\Delta f_q(x) = f_q^+(x) - f_q^-(x)$: Difference in Parton Density Functions of a polarized proton

σ_{ij} : unpolarized parton-parton scattering cross section (pQCD)

$\Delta\sigma_{ij}$: Difference in polarized parton-parton scattering cross section (pQCD)

$D(z,p_T)$: Fragmentation Function (perhaps spin dependent)

Transverse spin effect was expected to be very small for light quarks.

Yet, Nature Gives Us Large A_N

Fermi Lab, E704

$p_\uparrow + p \Rightarrow \pi + X$

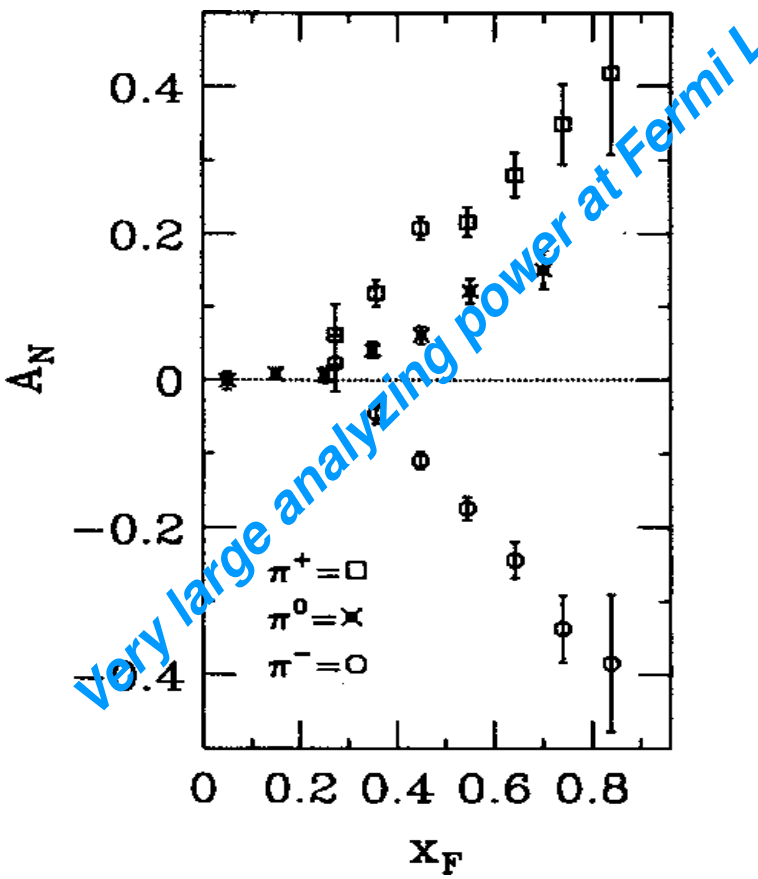

Very large analyzing power at Fermi Lab

√s=20 GeV, p_T=0.5-2.0 GeV/c:

π^0 E704, PLB261 (1991) 201.
$\pi^{+/-}$ E704, PLB264 (1991) 462.

RHIC, STAR

PRL 92, 171801 (2004)

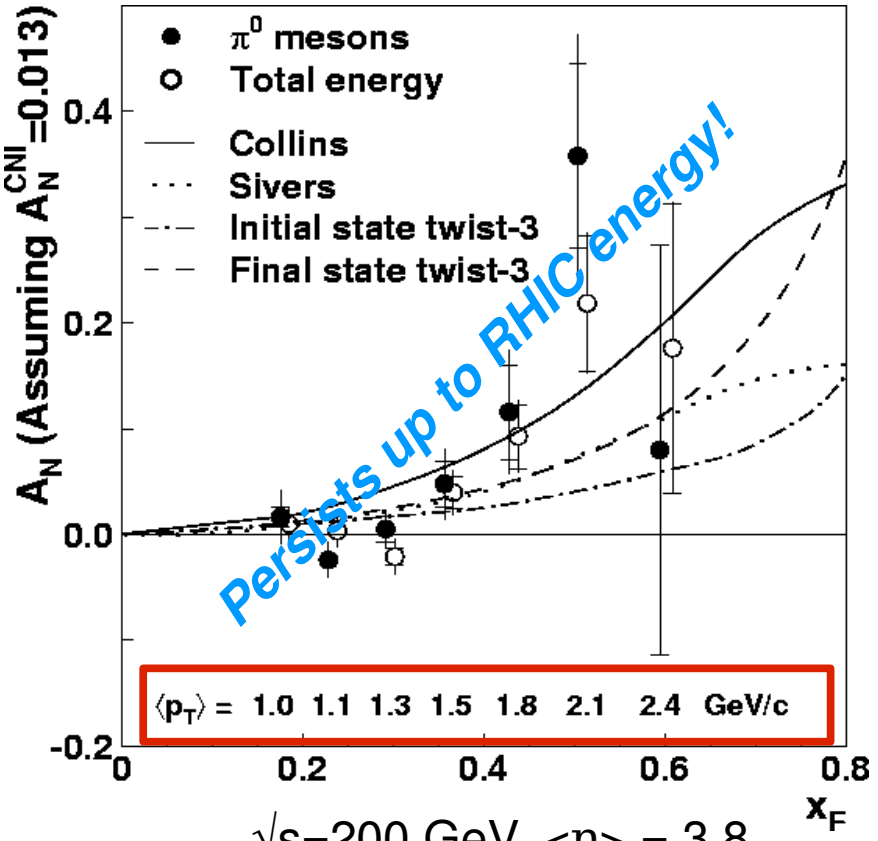

Persists up to RHIC energy!

√s=200 GeV, <η> = 3.8

Initial State Effect?
Final State Effect?
Higher Twist?

Initial State: Sivers Effect

A quark inside a proton may have orbital angular momentum that is correlated to the spin of the proton. If two quarks with opposite transverse momentum contribute different scattering amplitudes to the same final state, the transverse momentum of the quark can make the *proton → quark scattering sensitive to the transverse spin of the proton.* This process is referred to as the Sivers Effect. [Phys. Rev. D 41, 83 (1990); 43, 261 (1991)]

$$p + p \rightarrow \pi^0 + X$$

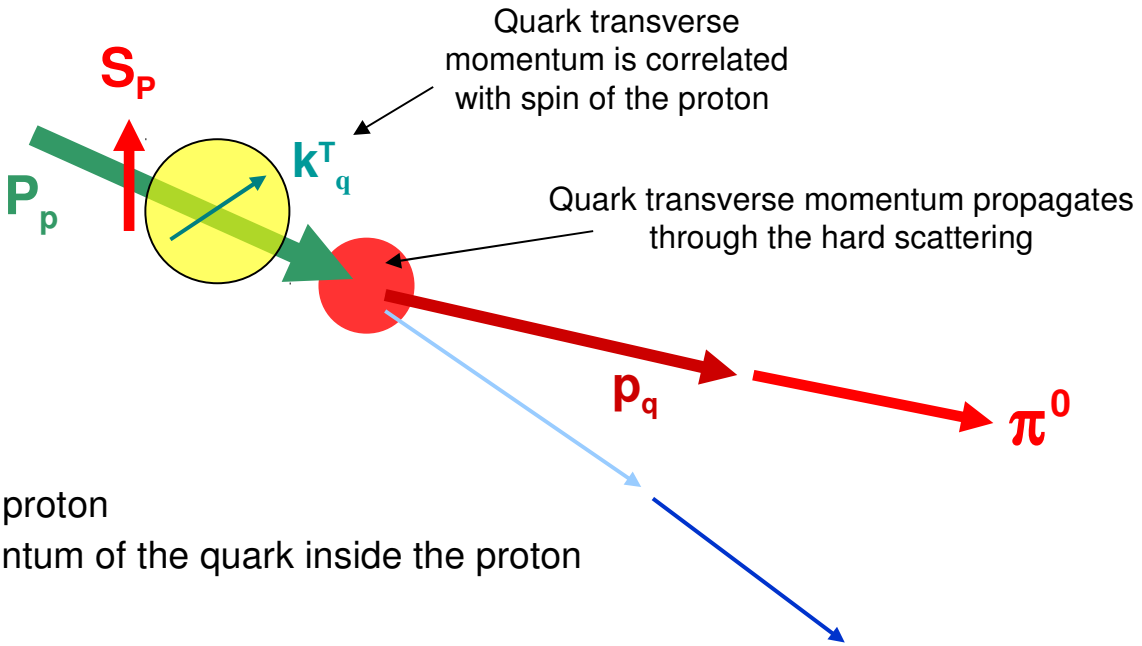

S_p = Spin of the proton
P_p = Momentum of the proton
k^T_q = Transverse momentum of the quark inside the proton

Hard scattering is not exactly collinear, which may be observed through di-jets and gamma-jets. Prompt photon can carry the asymmetry.

Final State: Collins Effect

Proton → quark scattering is insensitive to transverse spin. However, the quark retains its initial spin after a hard scattering, and *the quark → π^0 fragmentation can have azimuthal dependence on the transverse spin of the quark.* This process is referred to as the Collins Effect. [Nucl. Phys. B396, 161 (1993)]

$$p + p \rightarrow \pi^0 + X$$

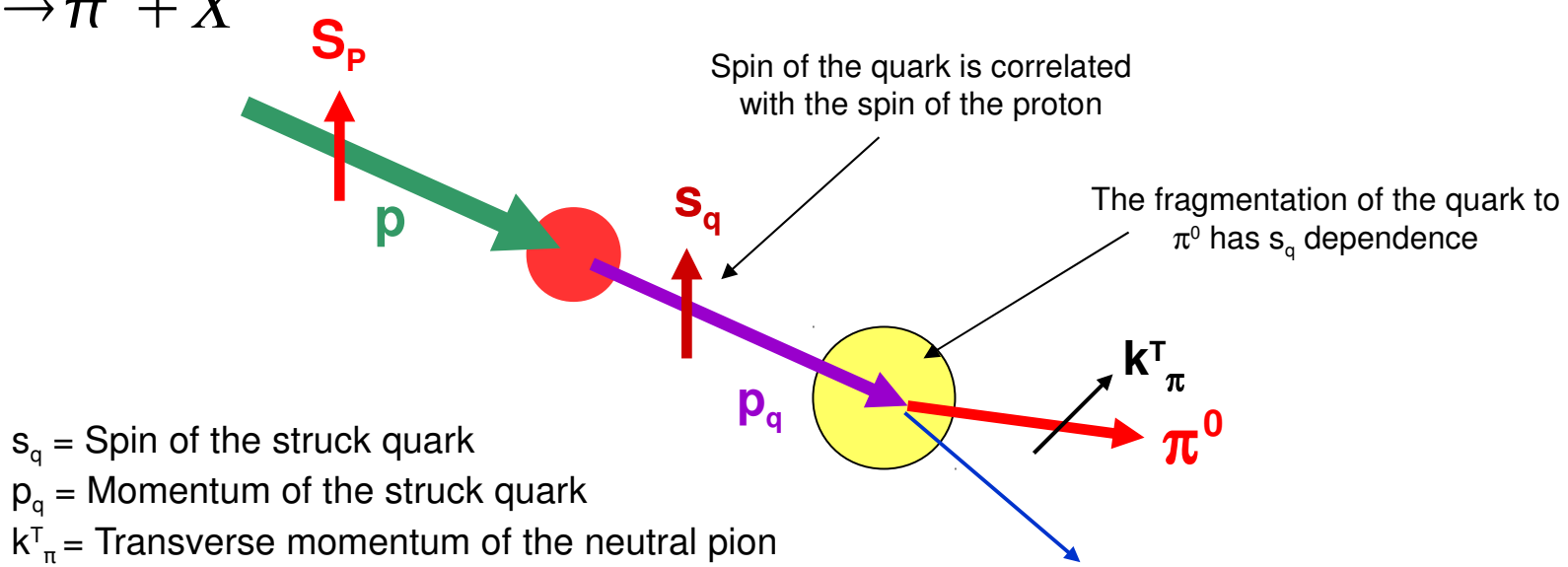

The asymmetry of the pion is with respect to the jet axis. There is no asymmetry for the jet axis. Hadronization is necessary for the asymmetry.

STAR Forward Pion Detector (FPD)

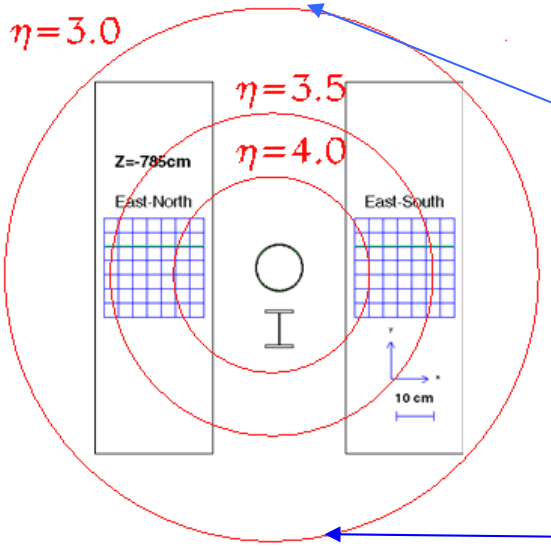

Run6 Configuration

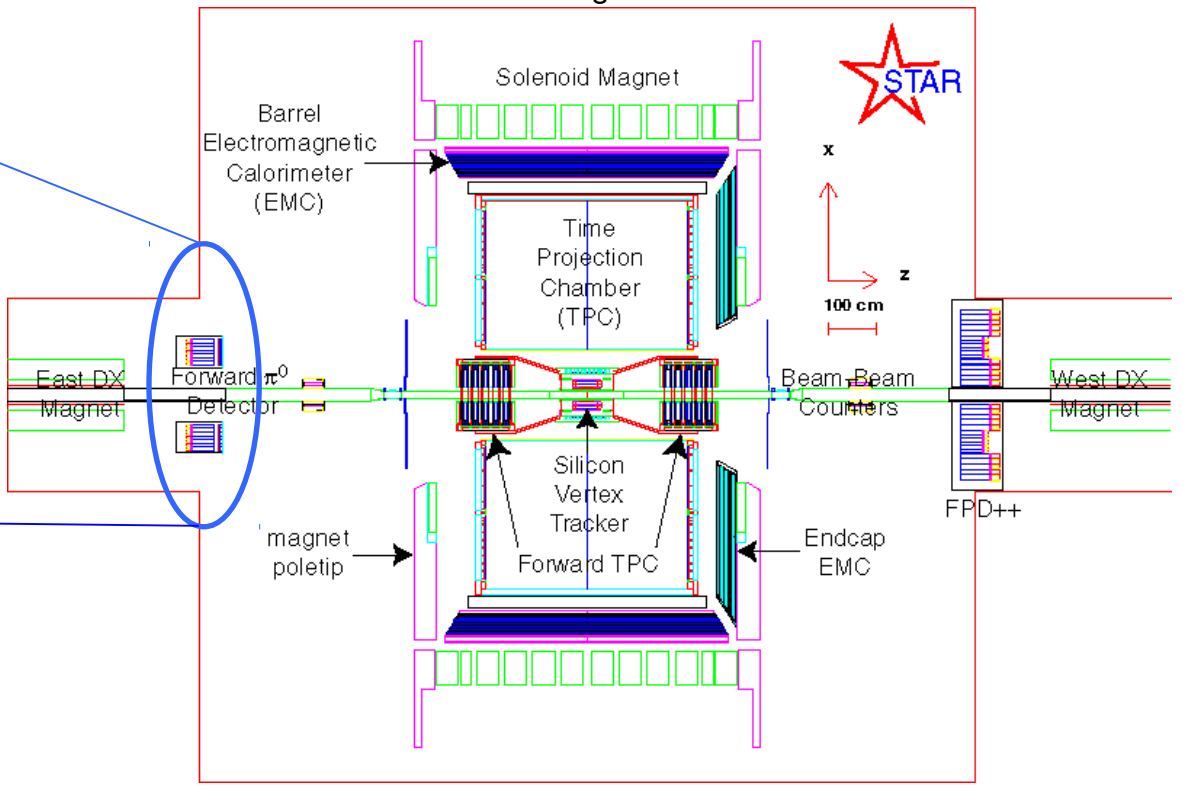

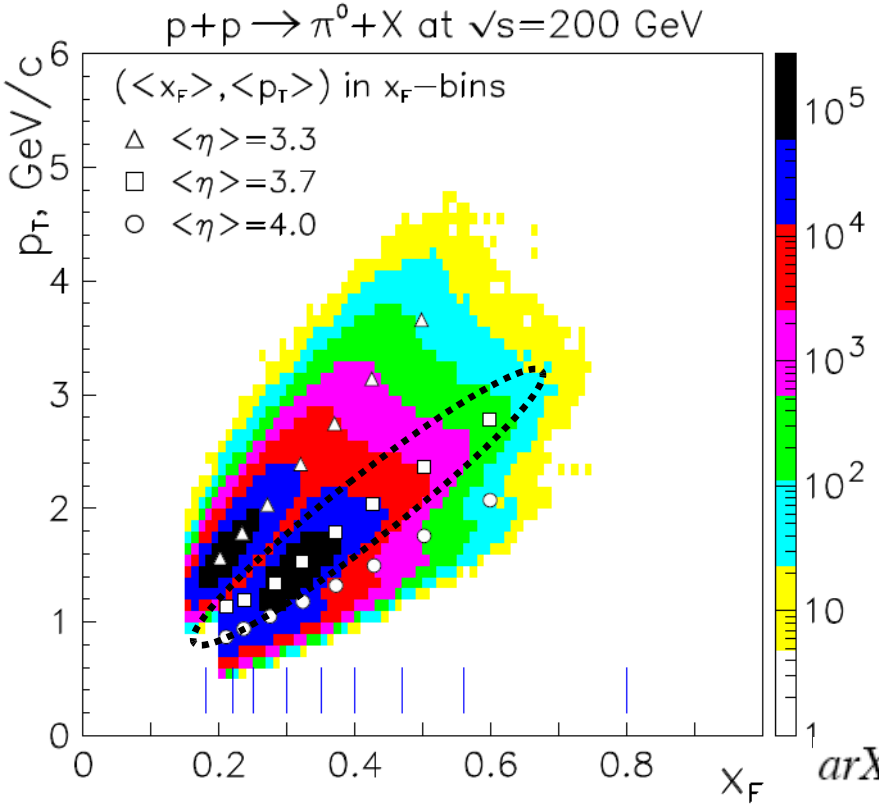

- STAR forward calorimeters have gone through significant upgrades since run3.
- In run6, the original FPD remained in the east, while the west FPD was expanded to FPD++.
- The east FPD consists of two 7X7 Pb-glass modules, EN and ES. During run6, it was placed at the “far” position. (x-offset~30cm, <η>~3.7)

arXiv:0801.2990v1 [hep-ex]

Forward π^0 Cross-Section

At $\sqrt{s}$=200GeV, π^0 cross-section measured by STAR FPD is ***consistent with the NLO pQCD calculation.*** Results at $\langle\eta\rangle$=3.3 and $\langle\eta\rangle$=3.8 have been included in the DSS global pion fragmentation function analysis. *(Phys.Rev.D75(2007) 114010)*

RHIC Run 2, Prototype FPD

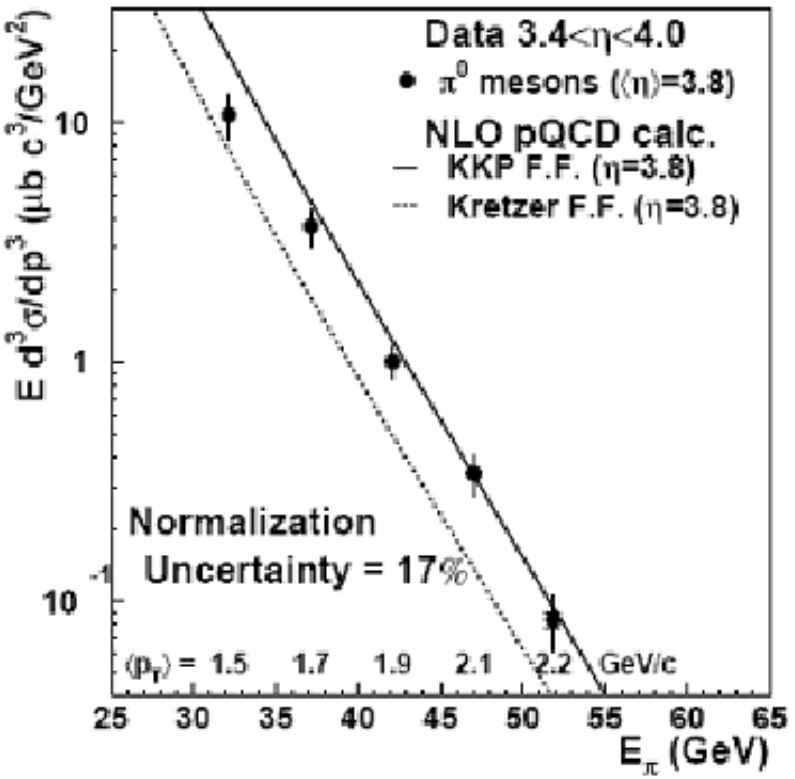

Phys. Rev. Lett. 92, 171801 (2004)

RHIC Run 3~6, FPD

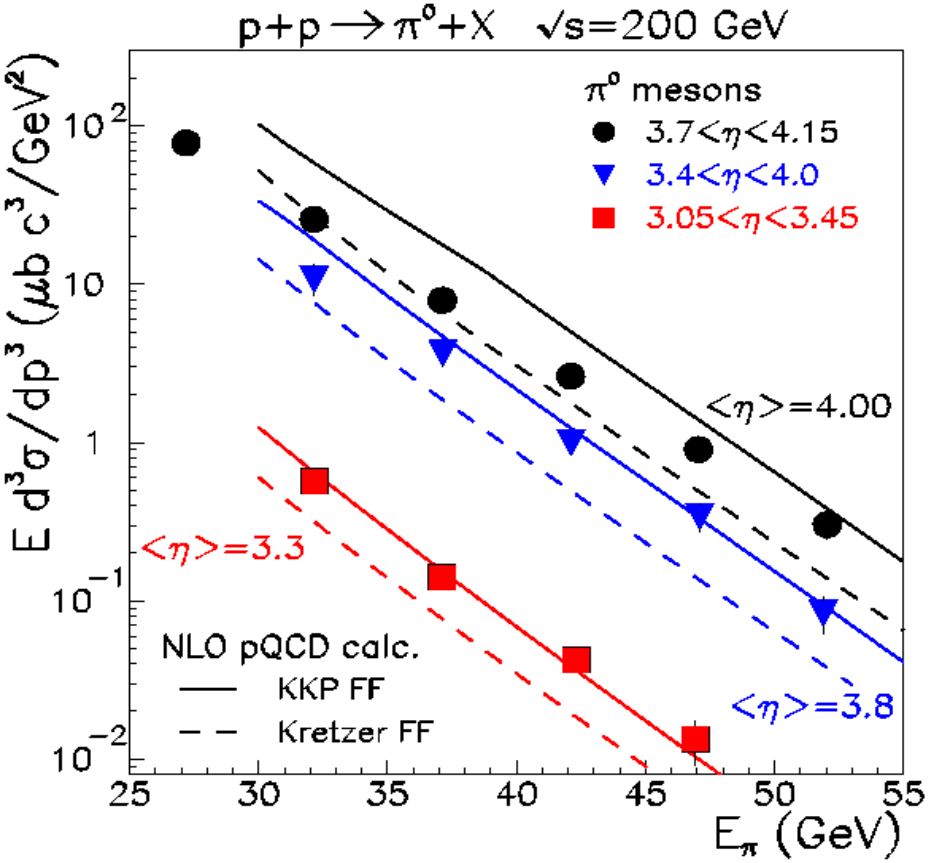

Phys. Rev. Lett. 97 (2006) 152302

Forward π^0 Single Spin Asymmetry

In the kinematic region where we measured the cross-section, STAR FPD has found a ***large transverse single spin asymmetry, A_N.***

$$A_N = \frac{d\sigma_\uparrow - d\sigma_\downarrow}{d\sigma_\uparrow + d\sigma_\downarrow} \simeq \frac{1}{P}\frac{\sqrt{N_\uparrow S_\downarrow} - \sqrt{N_\downarrow S_\uparrow}}{\sqrt{N_\uparrow S_\downarrow} + \sqrt{N_\downarrow S_\uparrow}}$$

RHIC Run 2, Prototype FPD

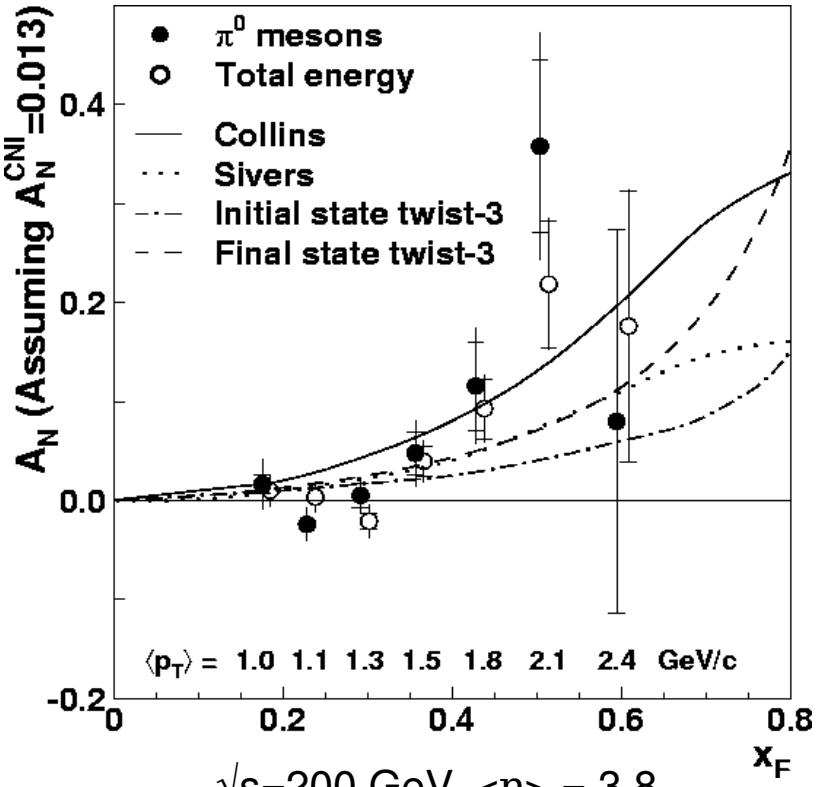

√s=200 GeV, <η> = 3.8

Phys. Rev. Lett. 92, 171801 (2004)

RHIC Run 3~6, FPD

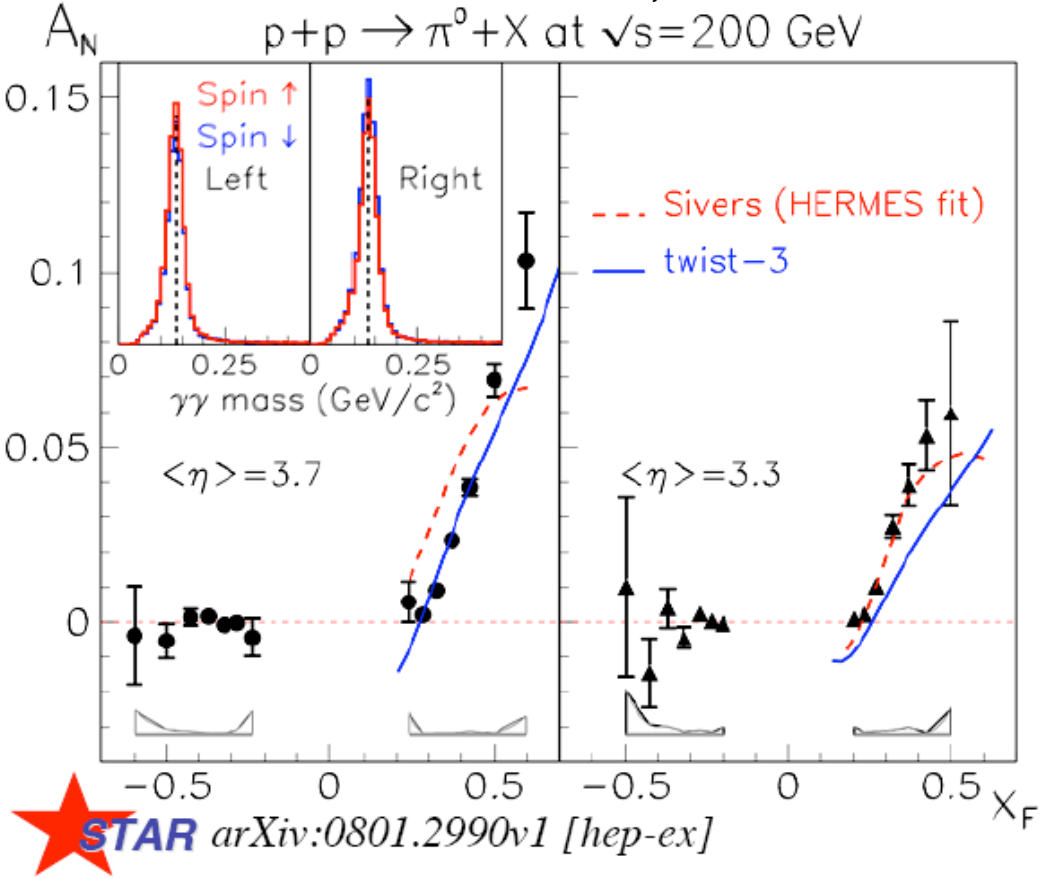

Phys.Rev.Lett.101, 222001 (2008)

p_T Dependence of A_N

For Fixed X_F, the asymmetry A_N does not fall with p_T as predicted by models, and perhaps expected on very general grounds.

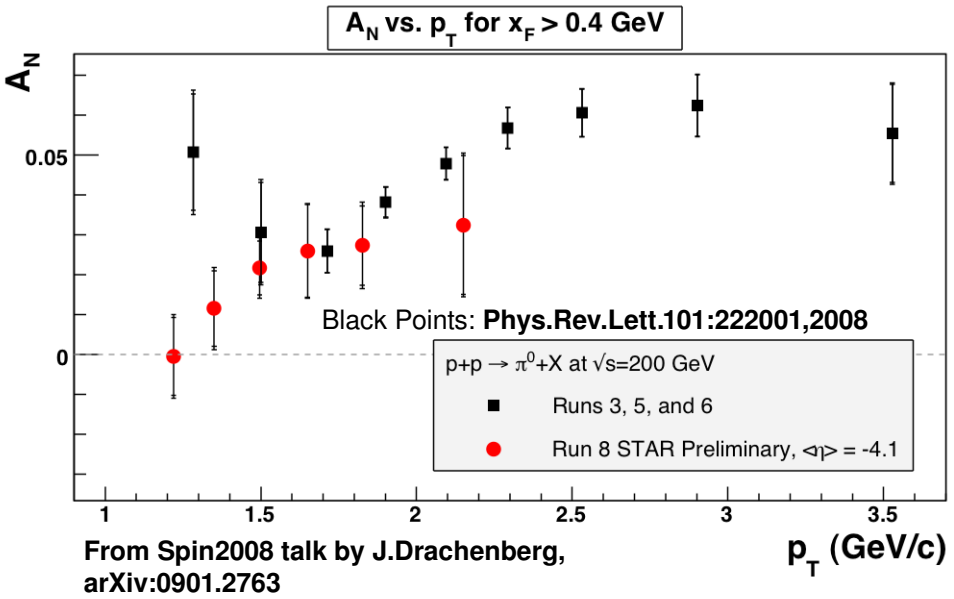

From Spin2008 talk by J.Drachenberg, arXiv:0901.2763

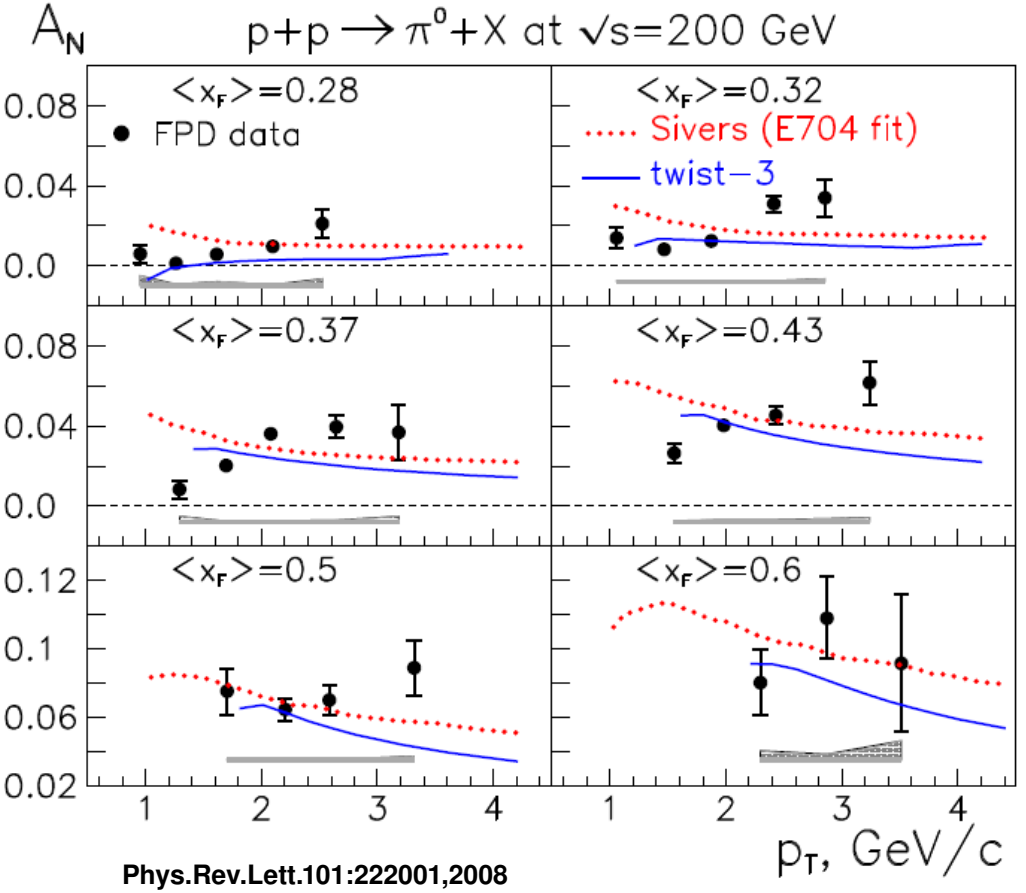

Phys.Rev.Lett.101:222001,2008

U. D'Alesio, F. Murgia, Phys. Rev. D **70**, 074009 (2004).
J. Qiu, G. Sterman, Phys. Rev. D **59**, 014004 (1998).

A_N rises as a function of p_T up to p_T of 2.5GeV of higher, a trend confirmed by the later RHIC Run 8 measurement. (RED)

Binning in x_F where each bin has roughly constant x_F does not alter this trend significantly.

p_T Dependence in Calculations of A_N

Sivers Effect / Collins Effect

Introduce transverse ***spin dependent offsets in transverse momentum independent of the hard scattering*** (definition of factorization).

$$p_T \Rightarrow p_T \pm k_T \quad (k_T \ll p_T)$$

"±" depending on the sign of proton transverse spin direction. ***This small offset, coupled to rapidly falling cross-section in p_T, can generate large asymmetry.***

Using STAR measured cross section form:

$$d\sigma_\uparrow \sim \frac{1}{(p_T - k_T)^6} \qquad d\sigma_\downarrow \sim \frac{1}{(p_T + k_T)^6}$$

$$A_N = \frac{d\sigma_\uparrow - d\sigma_\downarrow}{d\sigma_\uparrow + d\sigma_\downarrow} \sim \frac{6k_T}{p_T} + O\left(\frac{k_T}{p_T}\right)^2$$

Higher Twist Effect

Qiu, Sterman Phys. Rev. Lett **67,** 2264 (1991) etc.
Kouvaris et. al. Phys. Rev. D **74,** 114013 (2006)

A_N Fall as $1/P_T$ as required the by definition of higher twist.

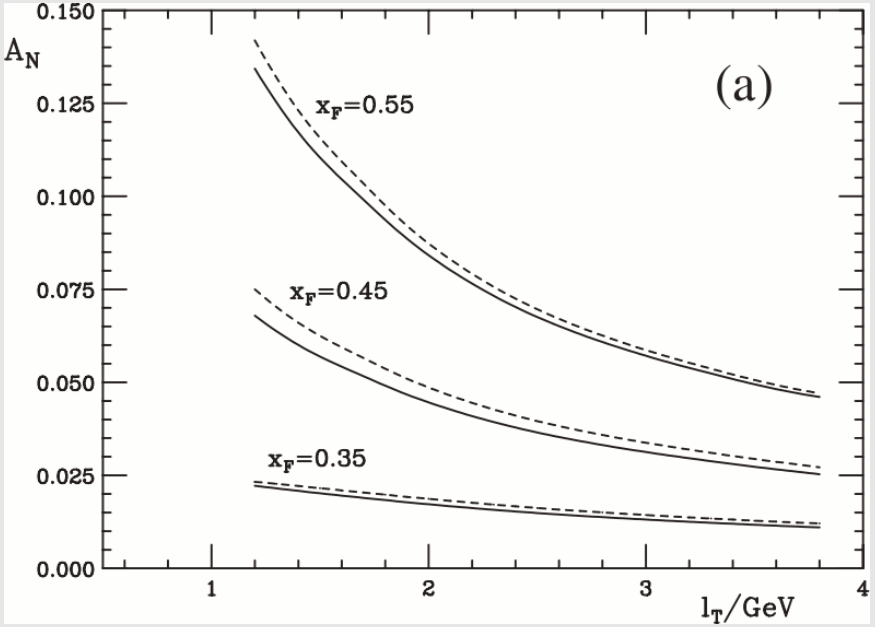

All of these models lead to $A_N \propto 1/p_T$

Forward Eta A_N: FNAL E704

Nominally (perhaps not significantly) larger asymmetry at high x_F for Eta than π^0. Large Uncertainty in Eta A_N.

$$p_\uparrow + p \rightarrow M + X$$
$$\bar{p}_\uparrow + p \rightarrow M + X$$

$$A_N = \frac{d\sigma_\uparrow - d\sigma_\downarrow}{d\sigma_\uparrow + d\sigma_\downarrow}$$

FNAL E704 Collaboration/Nuclear Physics B 510 (1998) 3–11

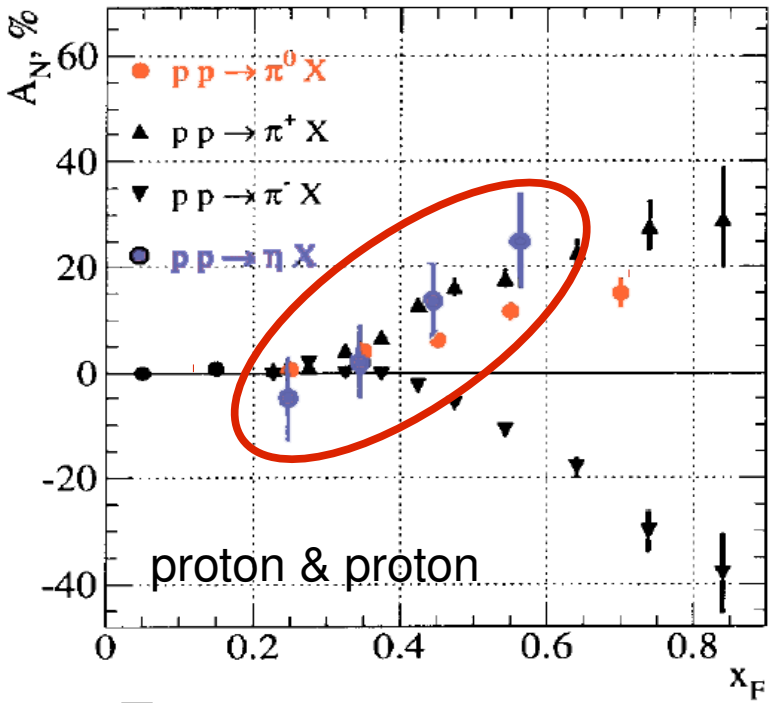

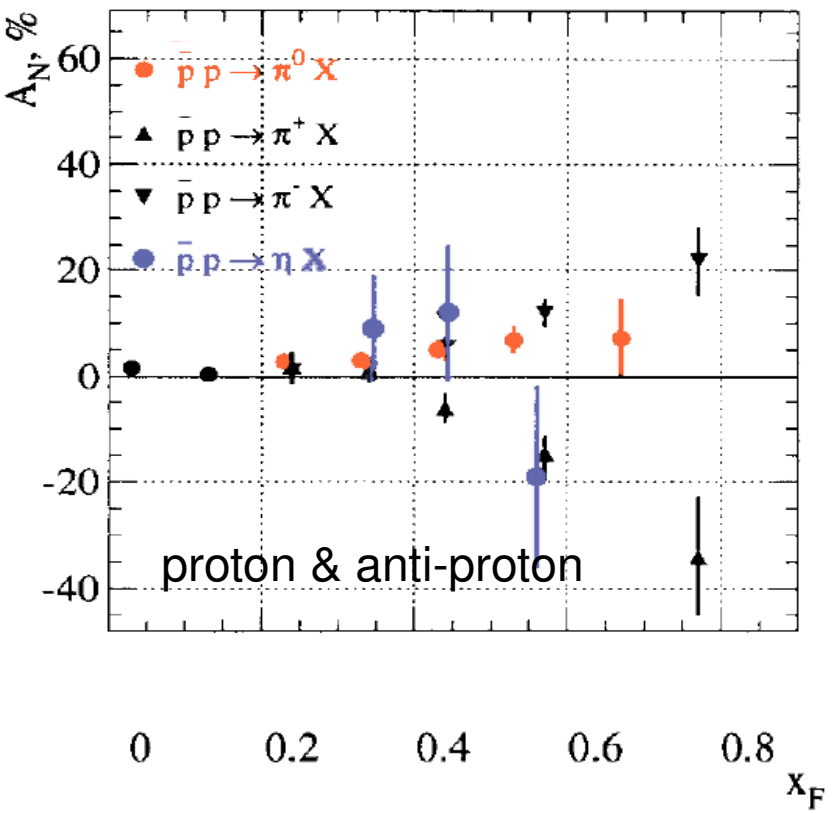

$$\sqrt{s} = 19.4 GeV \quad \langle p_T \rangle \sim 1 GeV/c$$

Eta Signal in Run6 FPD

Di-Photon Invariant Mass Spectra in 3 Energy Bins

- Center Cut
- 3 columns for 3 energy bins
- Each column shows a single plot in log and linear scale.

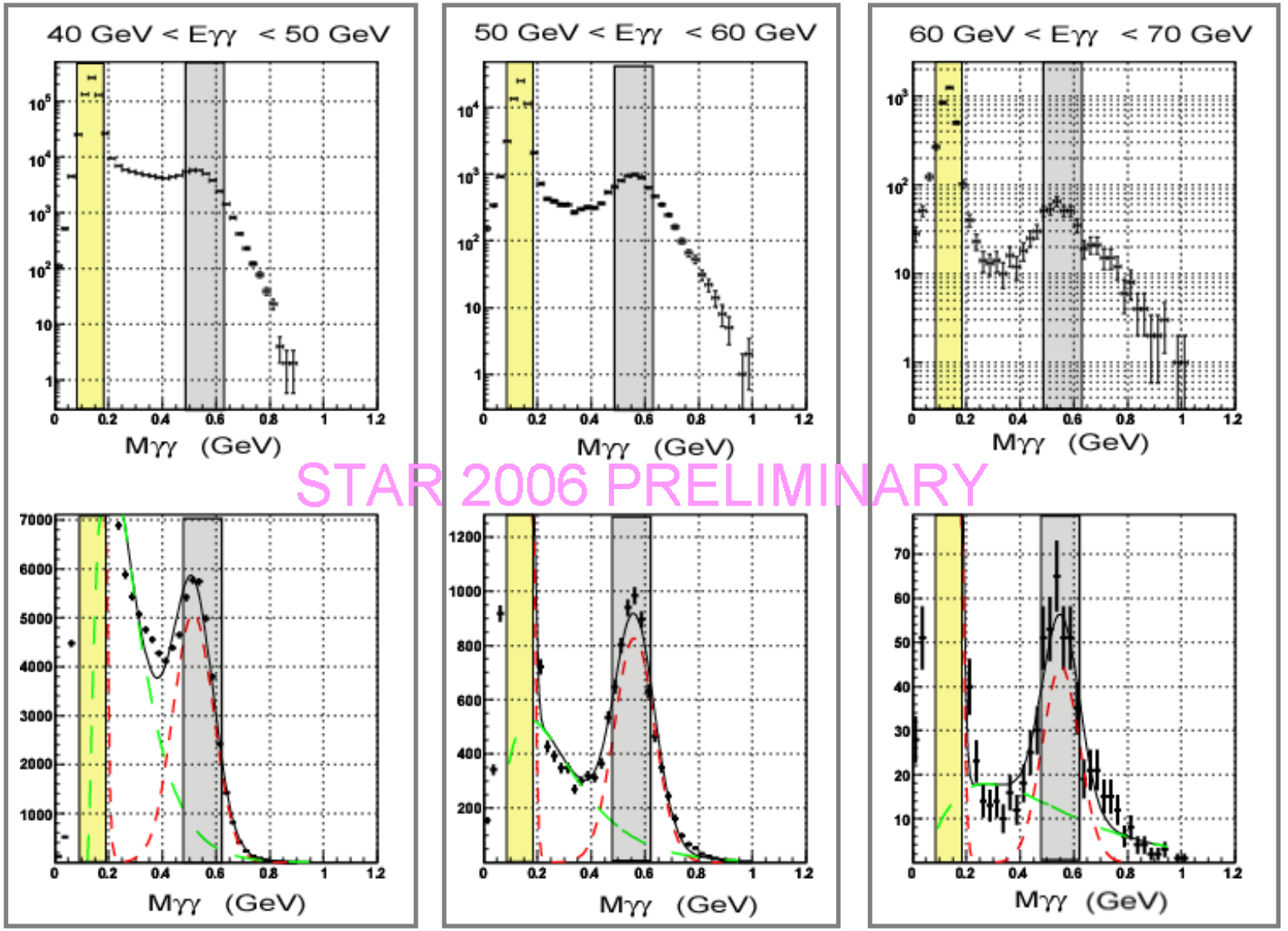

π^0 Mass Cut

$.085GeV < M_{\gamma\gamma} < .185GeV$

Eta Mass Cut

$.48GeV < M_{\gamma\gamma} < .62GeV$

$A_N(x_F)$ is reported for di-photon events in these two shaded mass regions. We do not separate contributions from backgrounds under the Eta and π^0 peaks.

Mass Dependence of A_N

$$p_{\uparrow} + p \rightarrow M + X \qquad \sqrt{s} = 200\,GeV$$
$$M \rightarrow \gamma + \gamma$$

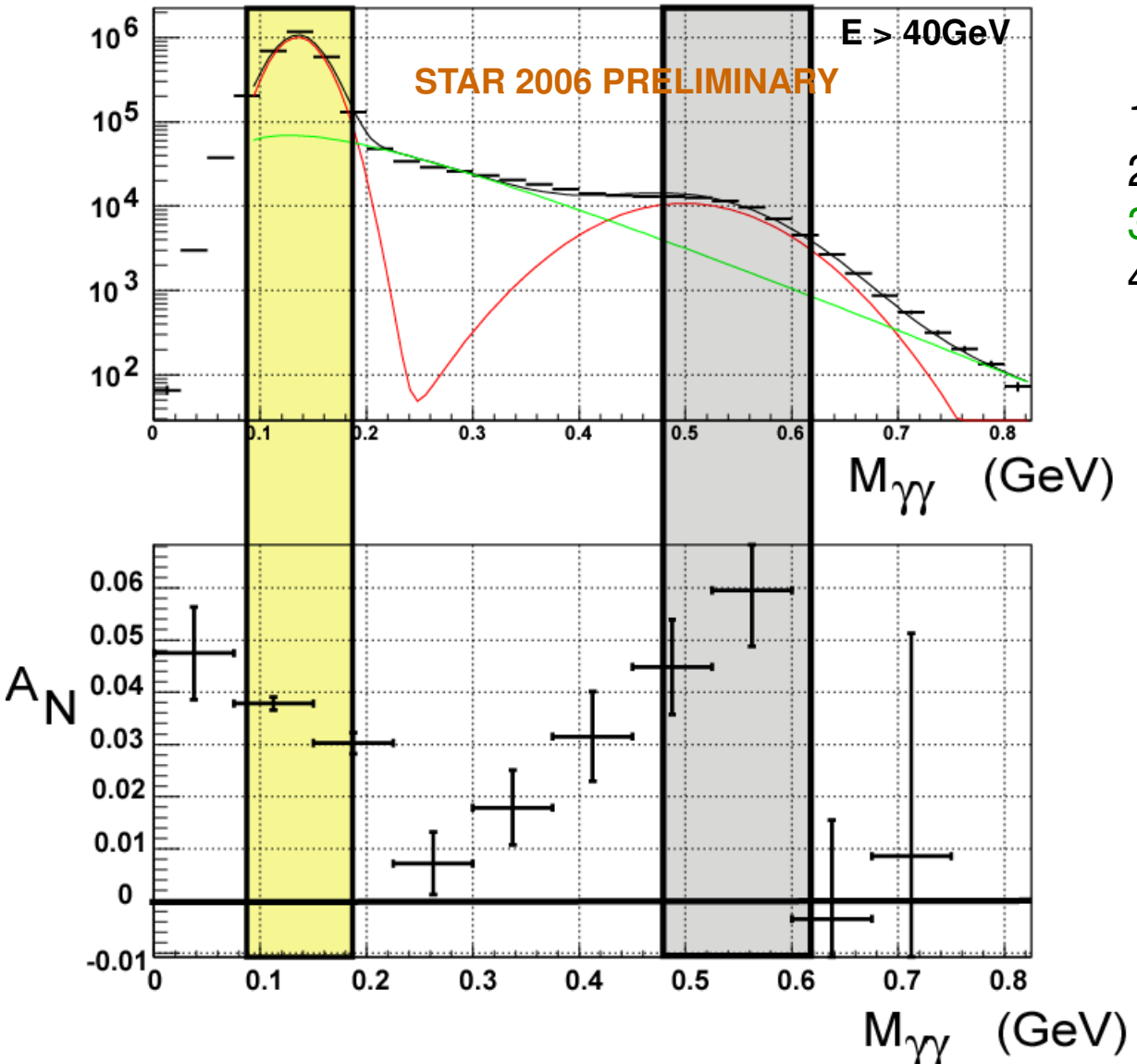

1. Nphoton = 2
2. Etotal > 40GeV
3. No Center Cut*
4. Average Beam Polarization = 56%

• Asymmetry clearly reveals the shape of two mass resonances.

• There is an "asymmetry valley" in between π^0 and Eta mass regions.

*Center Cut
→ $(\eta - 3.65)^2 + Tan(\phi)^2 < (0.15)^2$

$A_N(x_F)$ in π^0 and Eta Mass Regions

$$p_\uparrow + p \rightarrow M + X \qquad \sqrt{s} = 200\,GeV$$
$$M \rightarrow \gamma + \gamma$$

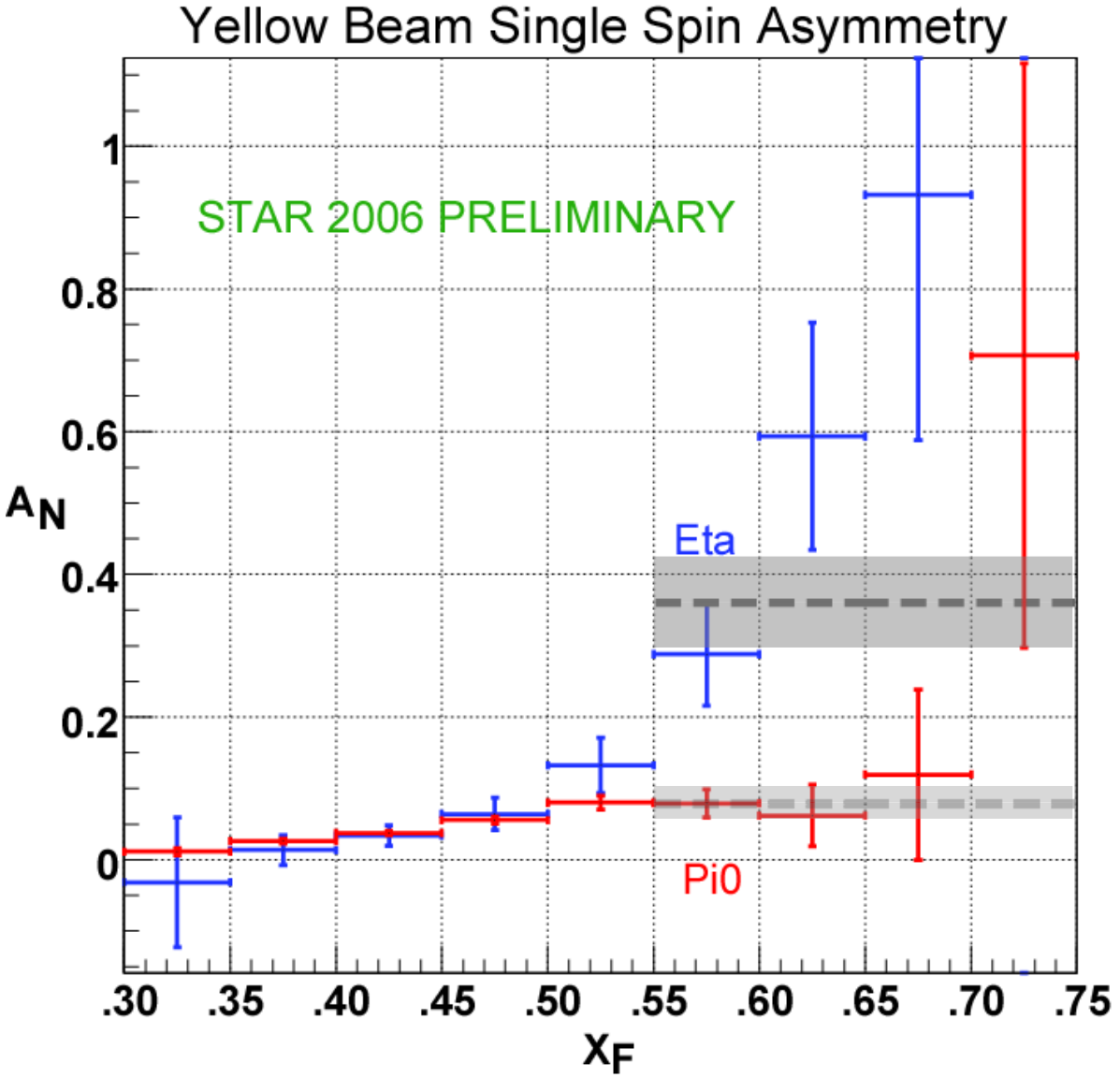

1. Nphoton = 2
2. Center Cut (η and ϕ)
3. Pi0 or Eta mass cuts
4. Average Beam Polarization = 56%

$$.55 < X_F < .75$$

$$\langle A_N \rangle_\eta = 0.361 \pm 0.064$$

$$\langle A_N \rangle_\pi = 0.078 \pm 0.018$$

For $0.55 < X_F < 0.75$, the asymmetry in the Eta mass region is greater than 5 sigma above zero, and about 4 sigma above the asymmetry in the π^0 mass region.

Len K. Eun

Could A_N be larger for η than π^0 ?

$$I=0 \begin{cases} \eta = \frac{1}{\sqrt{3}}(u\bar{u}+d\bar{d}+s\bar{s}) \\ \eta' = \frac{1}{\sqrt{6}}(u\bar{u}+d\bar{d}+2s\bar{s}) \end{cases}$$

$$I=1 \quad \{\pi^0 = \frac{1}{\sqrt{2}}(u\bar{u}-d\bar{d})$$

*Assume η,η' mixing angle: $\theta_p \sim -19.5\,degree$

Isospin difference?

- **Gluons** or **η** has **Isospin I=0**.
- **u quark** has **Isospin I=1/2**
- **π^0** has **Isospin I=1**.

- But we expect both mesons to come from **fragmentation of quark jets**.

- **For Sivers Effect:** Asymmetry is in the jet and should not depend on the details of fragmentation.

- **For Collins Effect**: Asymmetry reflects fragmentation of the quark jet into a leading **η** or **π^0** meson. Differences in fragmentation could relate to:

Mass difference?
Isospin difference?
Role of Strangeness?
But Collins Effect Should be suppressed when Z~1

More on Sivers and Collins

To generate the Sivers and/or Collins type asymmetry, we need two ingredients.

1. Extra k_T, small compared to p_T, that correlates with the spin of the proton

2. Rapidly falling cross-section in p_T

In essence, ***if the extra kT comes from the initial state, we get the Sivers effect, and if it comes from the final state, we get the Collins effect.***

For Sivers effect, the k_T cannot be different for π^0 and η, unless the two mesons come from different kinds of jets. This is probably not the case.

For Collins effect, in principal we don't know if k_T has to be the same for the two mesons. But, since $k_T \sim (1 - Z)p_T$, as $Z \rightarrow 1$ we get $k_T \rightarrow 0$ and therefore $A_N \rightarrow 0$. ***So Collins asymmetry should be suppressed at high Z.***

For both cases, ***it is possibly that the slope of the cross-section is different for π^0 and η in the kinematic region that we measured the A_N.*** This needs to be measured in the future.

Theory Score Card For Factorized QCD Picture for π^0 & η Transverse A_N

✓ Cross Section for π^0 agrees with PQCD (Normalization and Shape)

✓ Model calculations (Sivers, Collins, or Twist-3) can explain the x_F dependence of π^0 A_N

X Pt dependence of π^0 A_N. Inconsistent with $A_N \sim 1/p_T$

? Large difference in A_N between π^0 and η Can Collins or SIvers Model explain it?

? Ratio η / π^0 → nominal 40% - 50% Preliminary Result

Measuring Cross-sections for Large x_F π^0 and η

- **Previous π^0 cross-section measurement reached x_F of 0.55.** Around this point, the average separation between π^0 decay photons becomes less than 1 cell width. **Our η acceptance, however is mostly at x_F>0.5.**

- For the purposes of the spin measurement, our reconstruction algorithm proved to be adequate for x_F of up to 0.75. However, for the X-section measurement, substantial reworking was needed to achieve the required precision.

Incident angle effect → Geant based discrete projection
Improved π^0-γ separation → Based on cluster shape

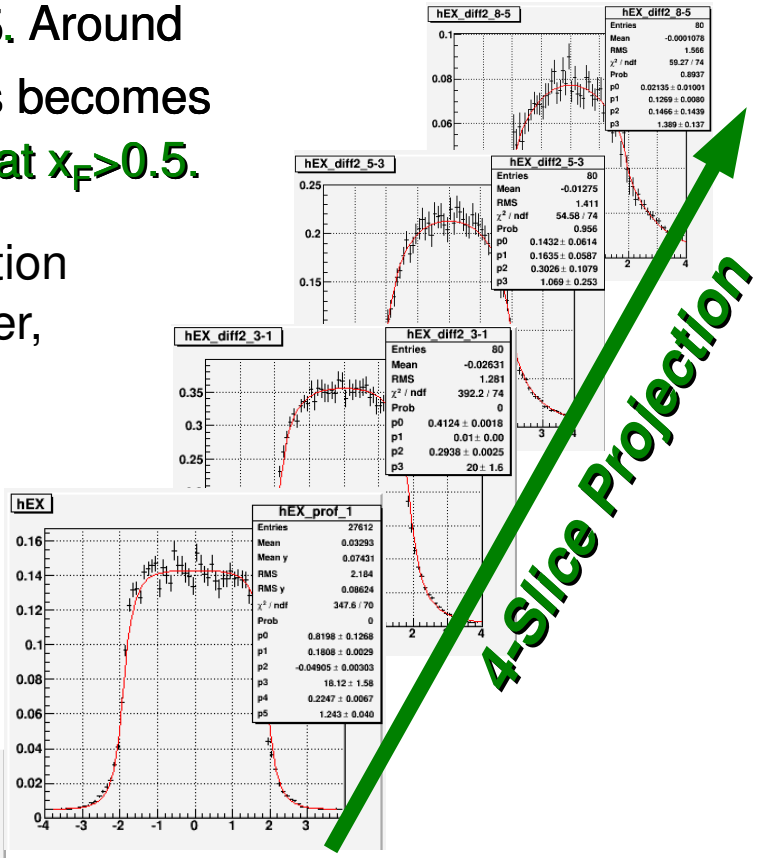

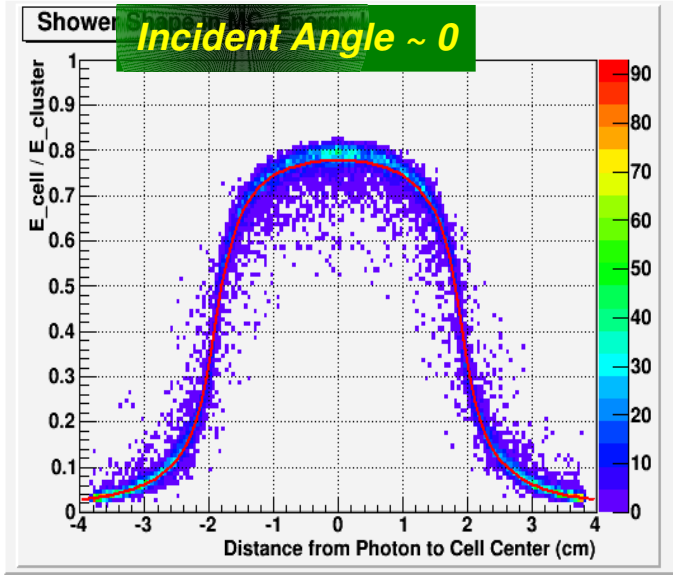

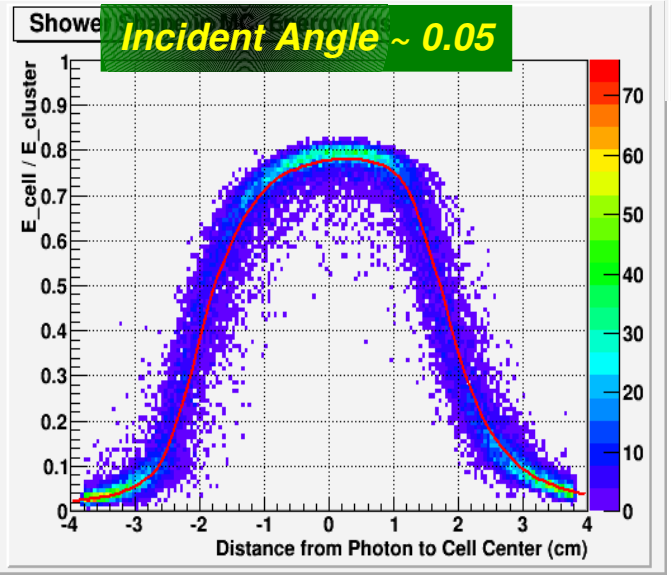

Incident angle correction significantly improves the photon position resolution.

π^0-γ Separation at High x_F

Single photon background for high-energy / small-separation π^0 signal
→ Potentially stronger prompt photon X-section at high x_F can aggravate it.

Linear E weighting

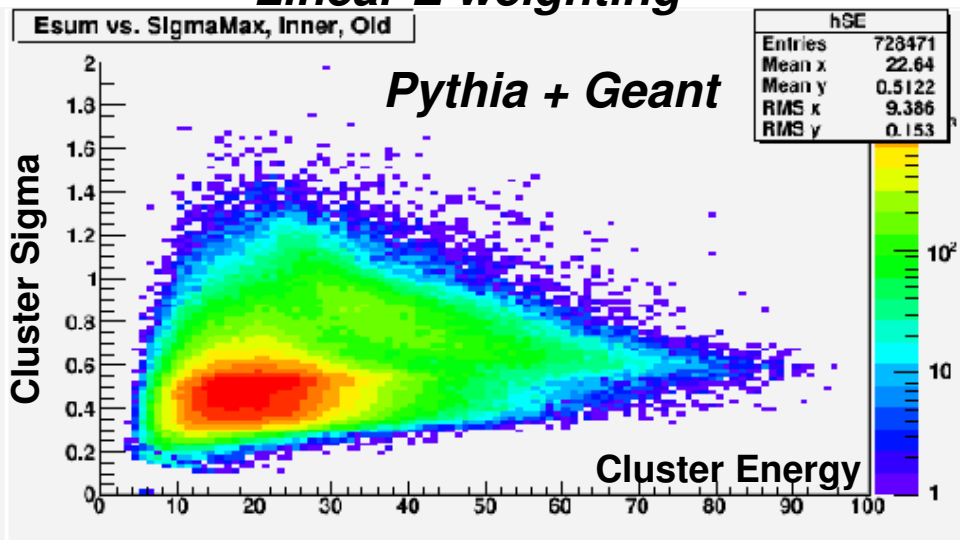

Originally, we used ***energy weighted 2nd moment of the cluster*** to separate π^0 candidates from prompt photon candidates.
→ Worked ok for x_F<0.5, but not so well for higher x_F.

Weighting with the log of energy, with an appropriate minimum energy cut, improves the separation dramatically.

Log E weighting

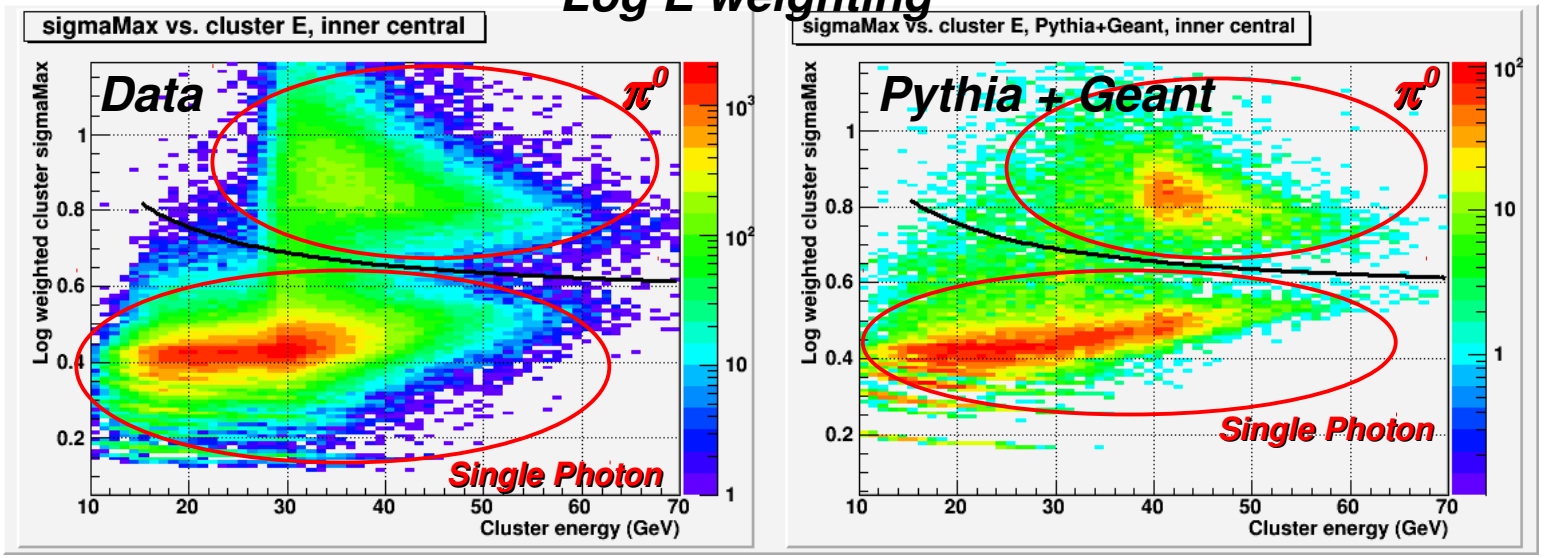

Data-MC Shower Shape Discrepancy

There is an apparent discrepancy in shower shape between the data and Geant.

1. Directly measured shower shape in data does not match Geant

2. Data exhibits energy dependent shift in π^0 mass, which is absent from Geant

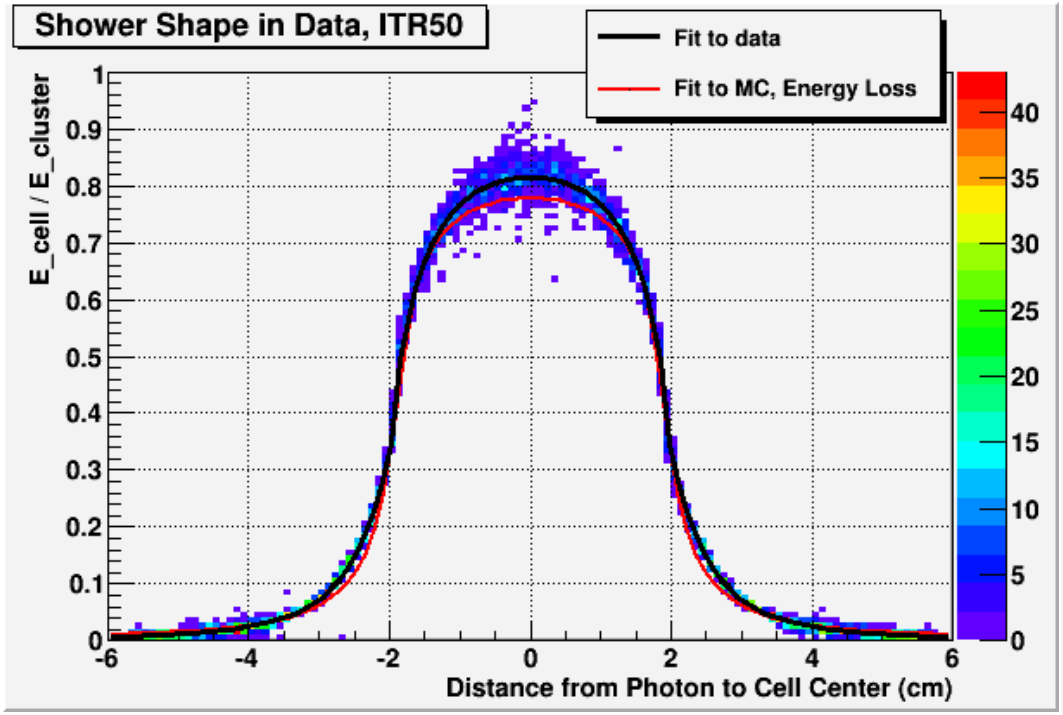

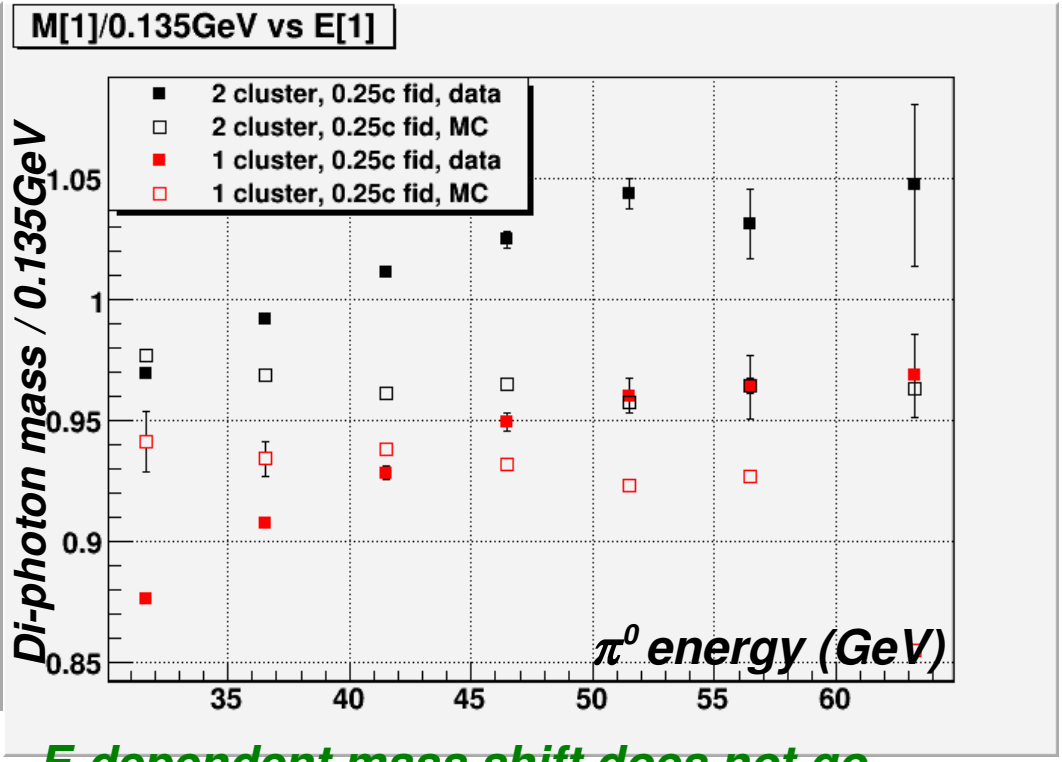

The shower shape in data is 4~5% narrower in the center than what we expect from MC.

E-dependent mass shift does not go away in the data even with well matched shower function.

→ Calibration relies on π^0 mass. This problem significantly limits our ability to calibrate.

Relative Energy Scale Systematics

The leading systematics for the X-section ratio analysis is **the relative energy scale between π^0 and η.**
→ Systematic cell by cell calibration non-uniformity is possible.
→ The two mesons populate somewhat different regions of the detector.

Photon Locations for π^0 and η with Epair > 55GeV

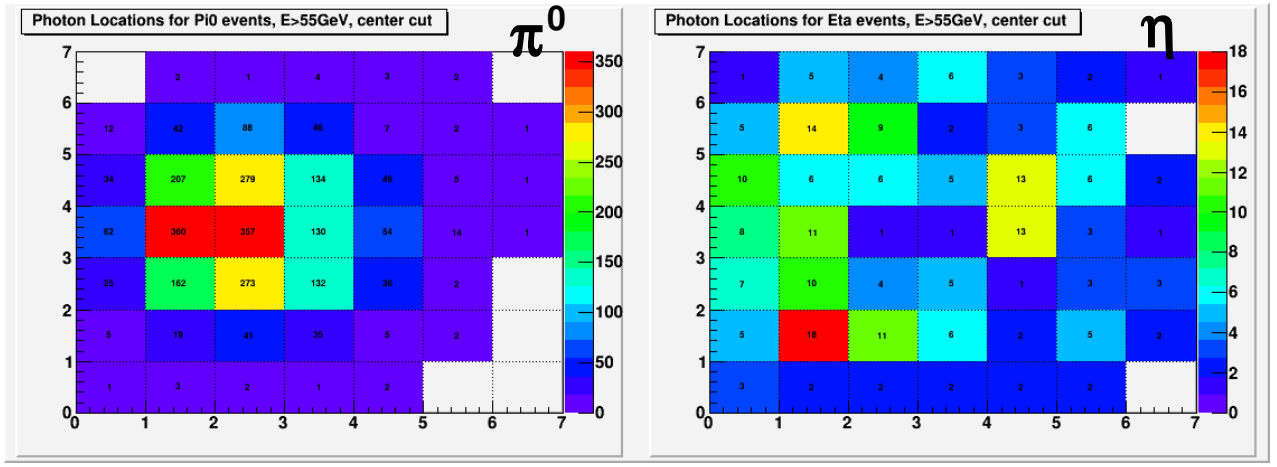

Evaluation of the Energy Scale Uncertainty

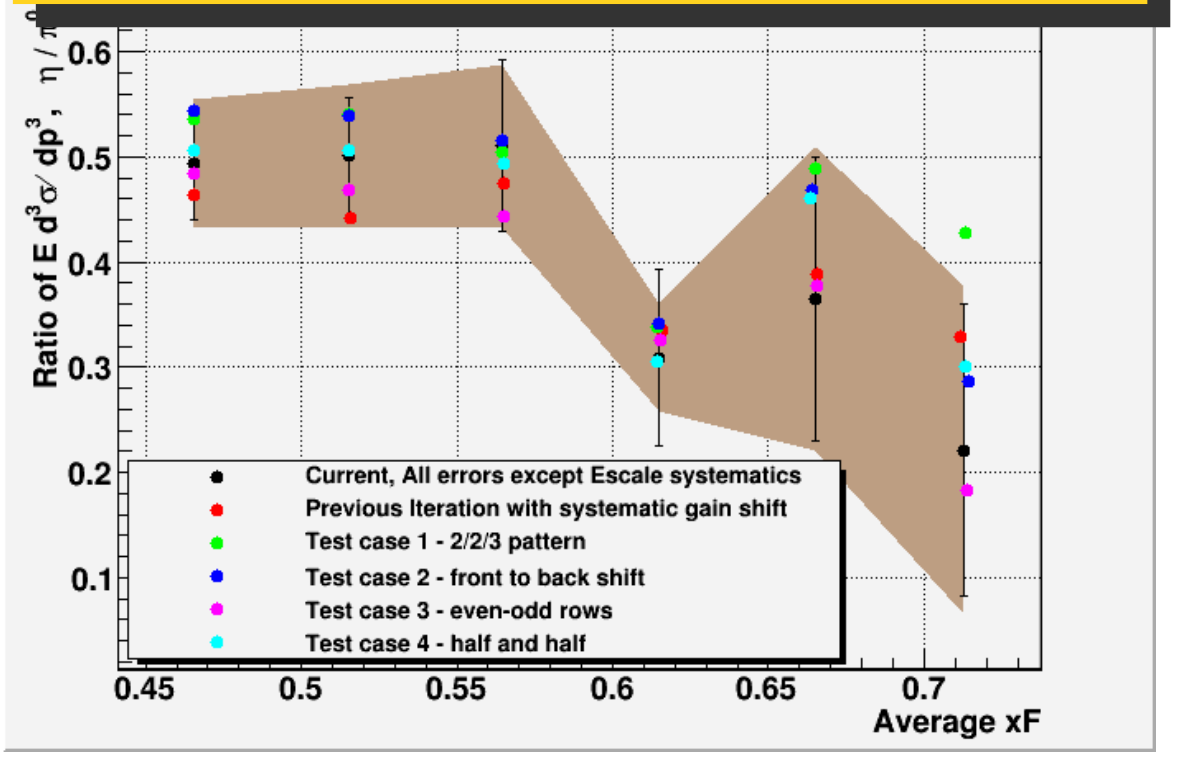

In order to estimate the effects of the gain non-uniformity including potential cancellations, we tried **artificially generated, severely pathological examples of the most likely patterns that could appear in the calibration.**

The X-section ratio was measured in each case, and the envelope for the energy scale systematics was determined.

Preliminary η / π^0 Cross-section Ratio

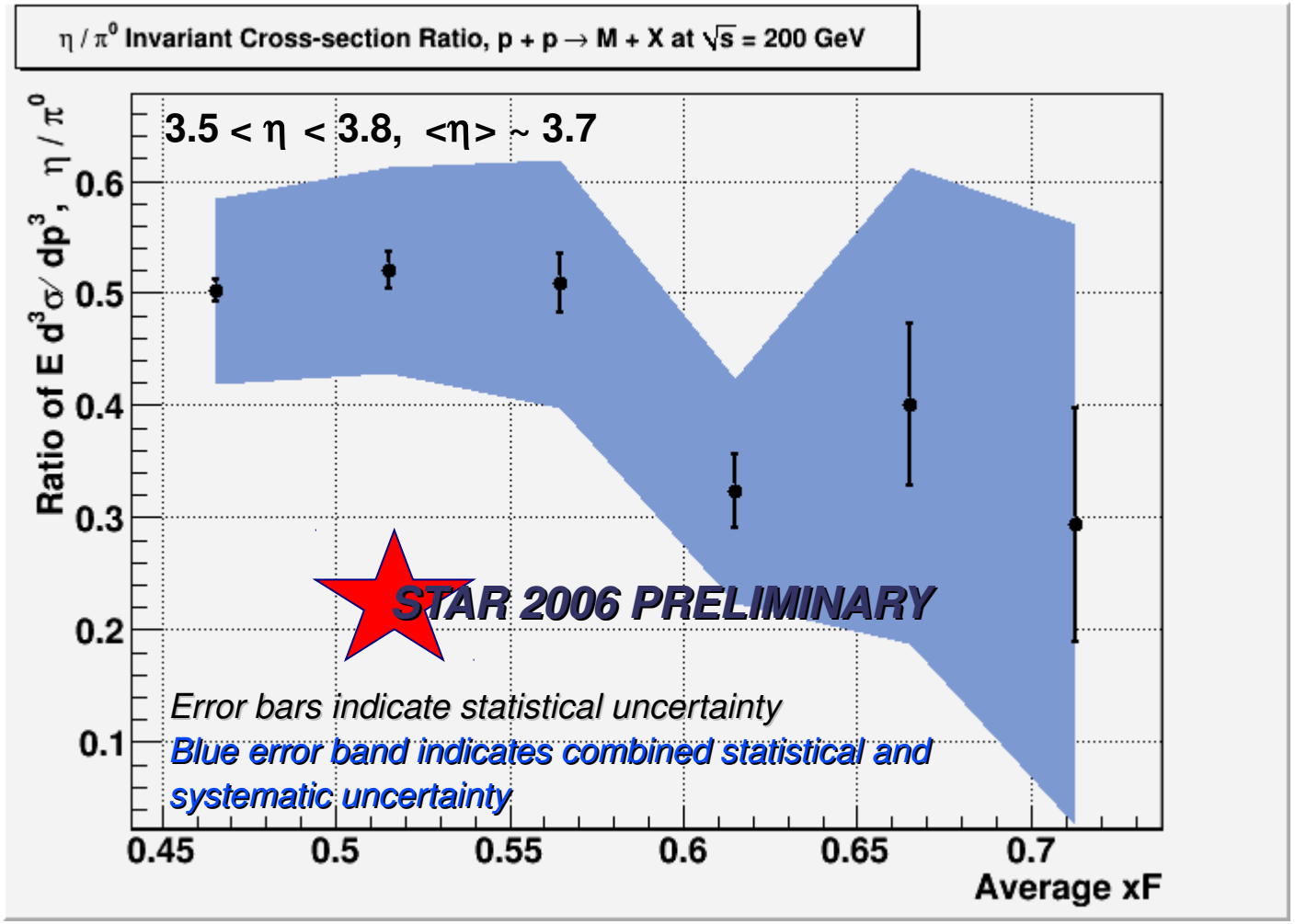

Points are plotted at the average x_F point for each bin, with a uniform bin size of 0.05 in x_F to make 6 bins from x_F of 0.45 to x_F of 0.75.

Cerenkov Based Shower Shape

FPD shower shape in Geant was based on charged particle energy loss, which tracks the shape of the shower. There isn't much we can do to change this shape.

Cerenkov based shower shape is naturally much narrower than even the data. From here, we can tune the absorption length in the Pb-glass, and the reflectivity of the Pb-glass and aluminized mylar interface to broaden the shape to match the data.
Cerenkov based shower also produces energy dependent gain shift, coming from the shift in shower max as a function of energy coupled to the attenuation of optical photons.

Mild modification to the published optical properties of the FPD produces very good match to data

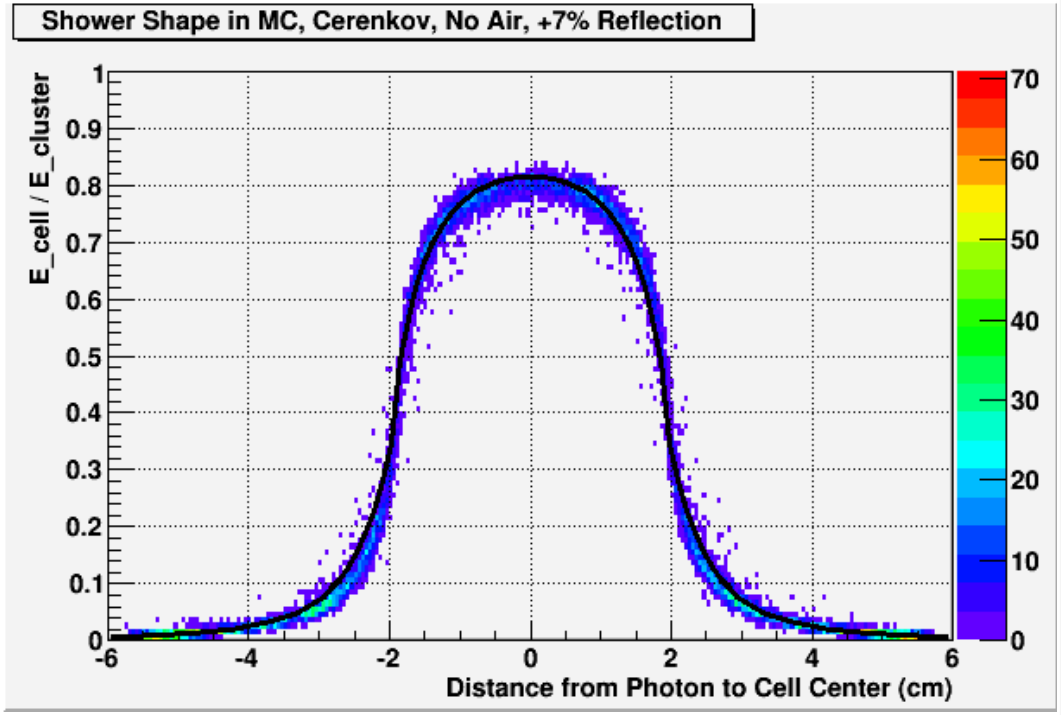

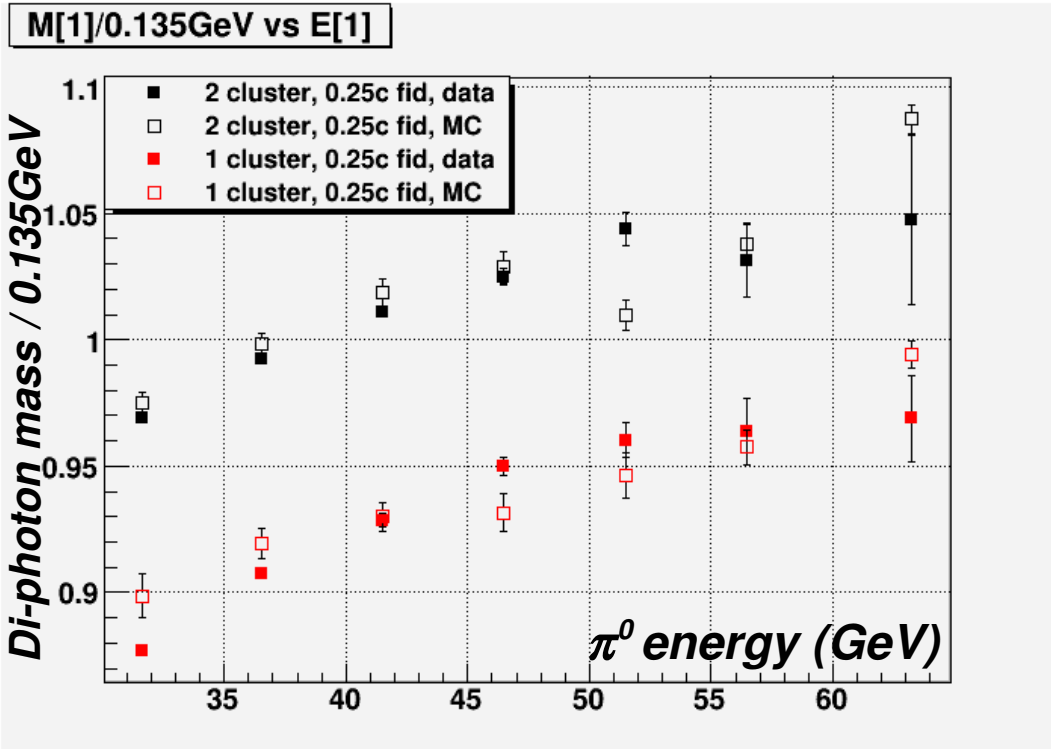

STAR Forward Meson Spectrometer (FMS)

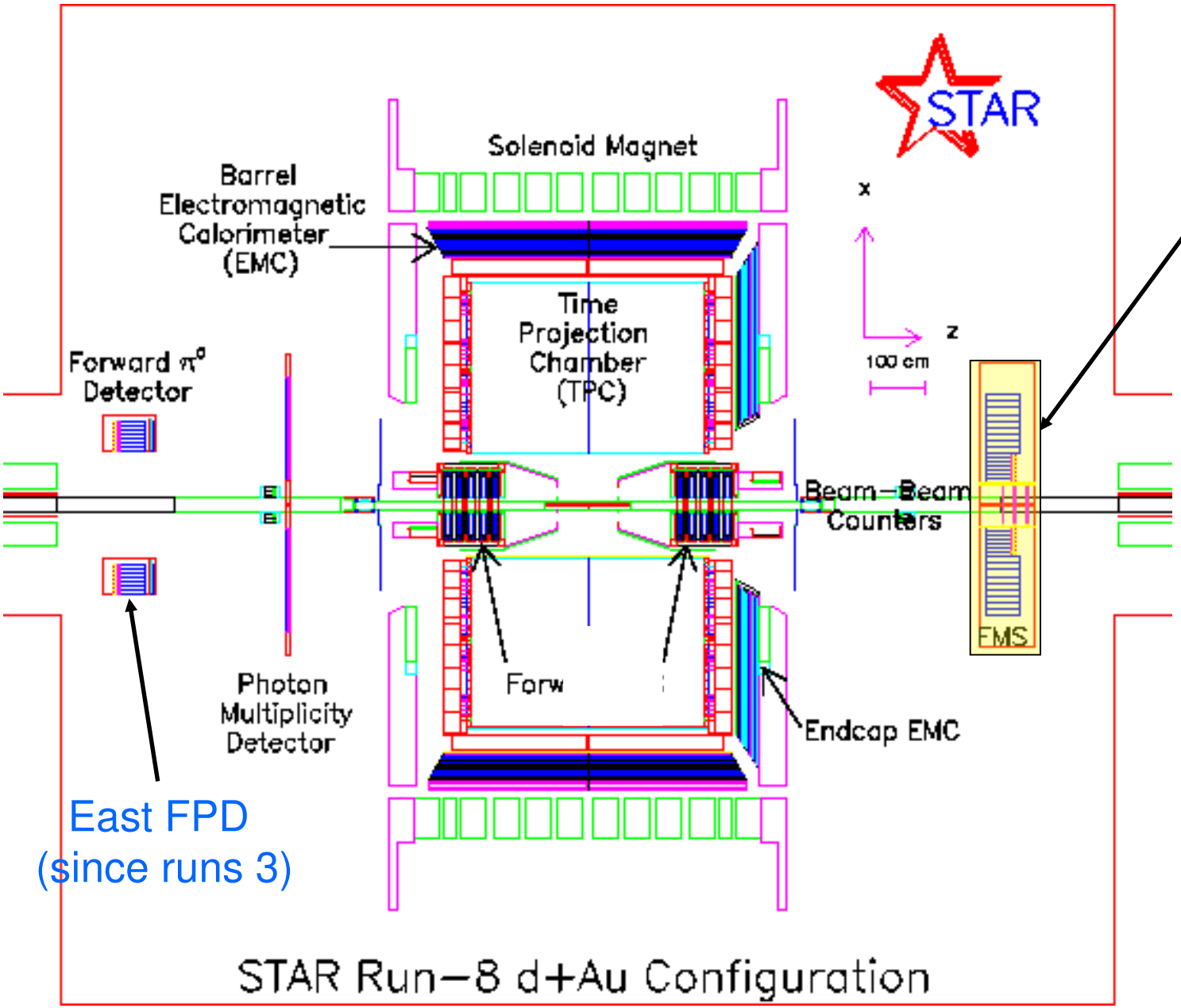

Since Run 8:
FMS

- Stack of 1264 lead glass cells, roughly 18 X_0 in z.
- Located at far West side of Hall, at the opening to RHIC tunnel. Faces blue beam.
- 7.5 meters from interaction point

Len K. Eun

STAR Forward Meson Spectrometer (FMS)

Run 2 ~ 6: FPD

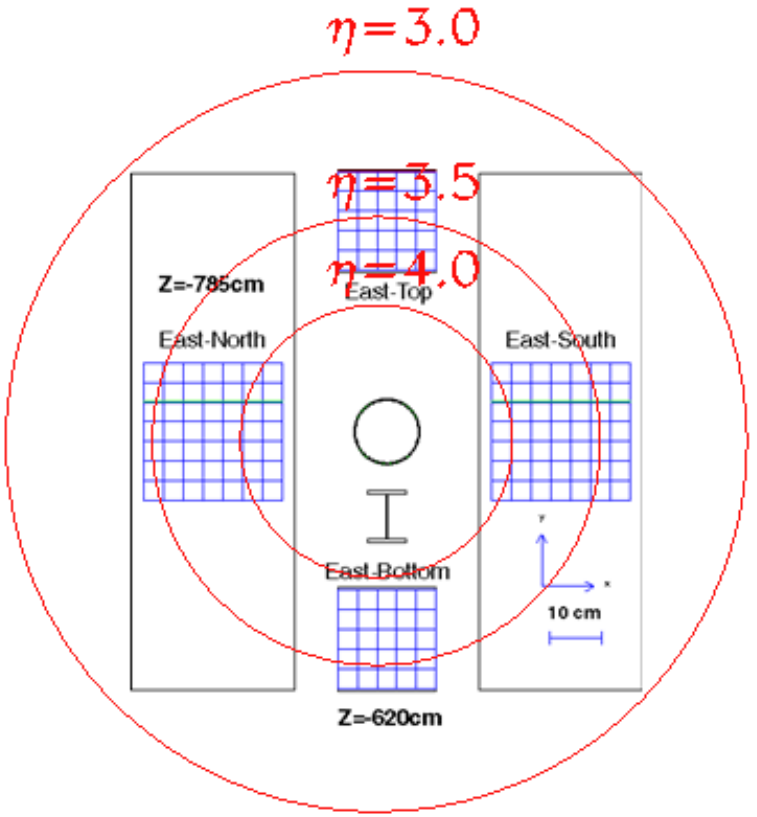

- FMS, along with EEMC and BEMC, provides nearly complete EM coverage from $-1 < \eta < +4$

- FMS allows the detection of nearside π pair, and Jet-like reconstruction → Collins effect

- In conjunction with the EEMC and BEMC, awayside jet can be identified → Sivers effect

- Other physics objectives include
  - Small x gluon saturation
  - Prompt photon
  - Drell Yan

STAR Forward Meson Spectrometer (FMS)

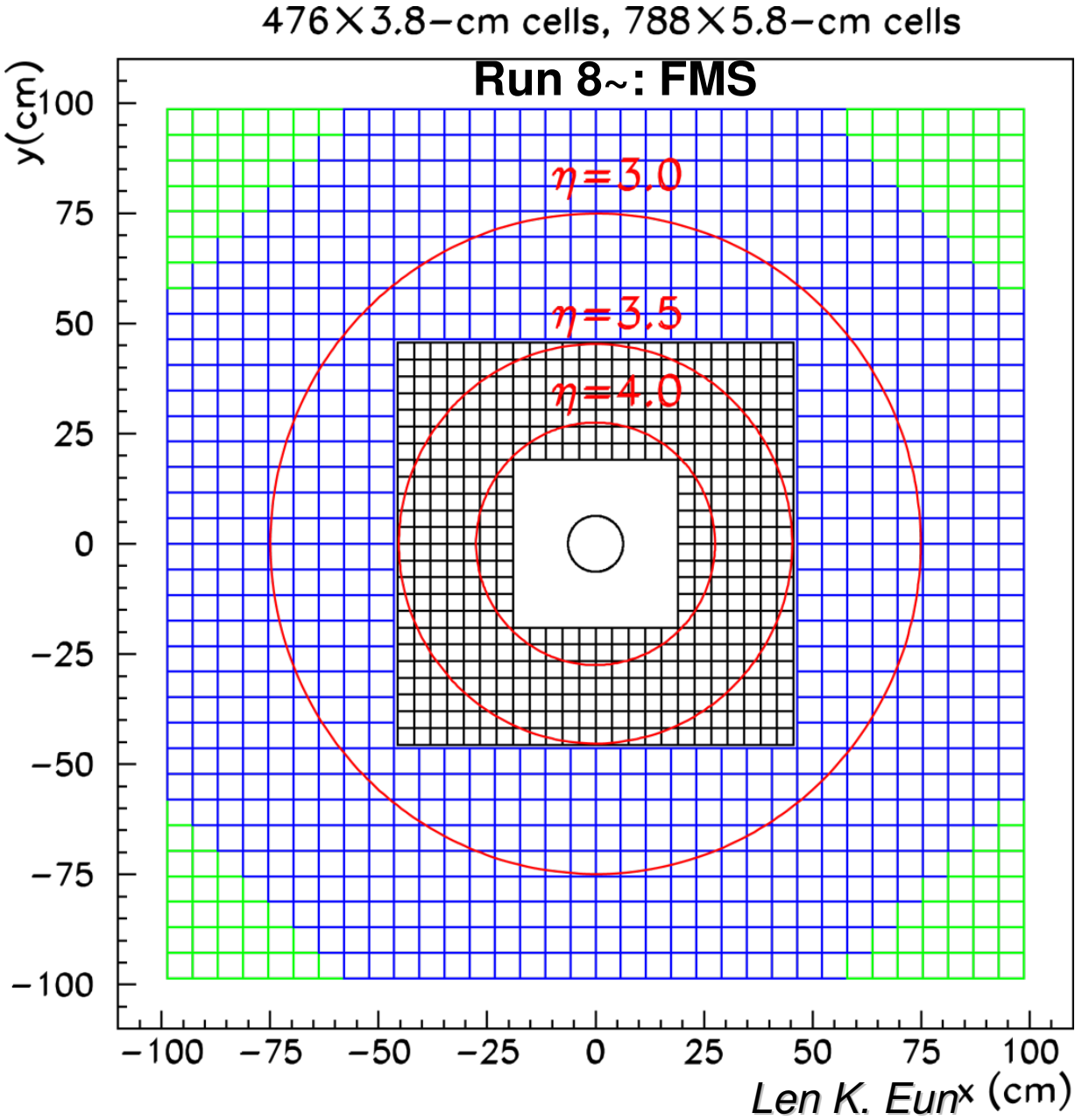

- FMS, along with EEMC and BEMC, provides nearly complete EM coverage from $-1 < \eta < +4$

- FMS allows the detection of nearside π pair, and Jet-like reconstruction → Collins effect

- In conjunction with the EEMC and BEMC, awayside jet can be identified → Sivers effect

- Other physics objectives include
  - Small x gluon saturation
  - Prompt photon
  - Drell Yan

FMS Greatly Enhances STAR EM Coverage

EM Calorimeters

BEMC	-1<η<1
eEMC	1<η<2
FMS	2.5<η<4
FPD	movable

Tracking

TPC	-1.2<η<1.2
FTPC	2.8<η<3.8

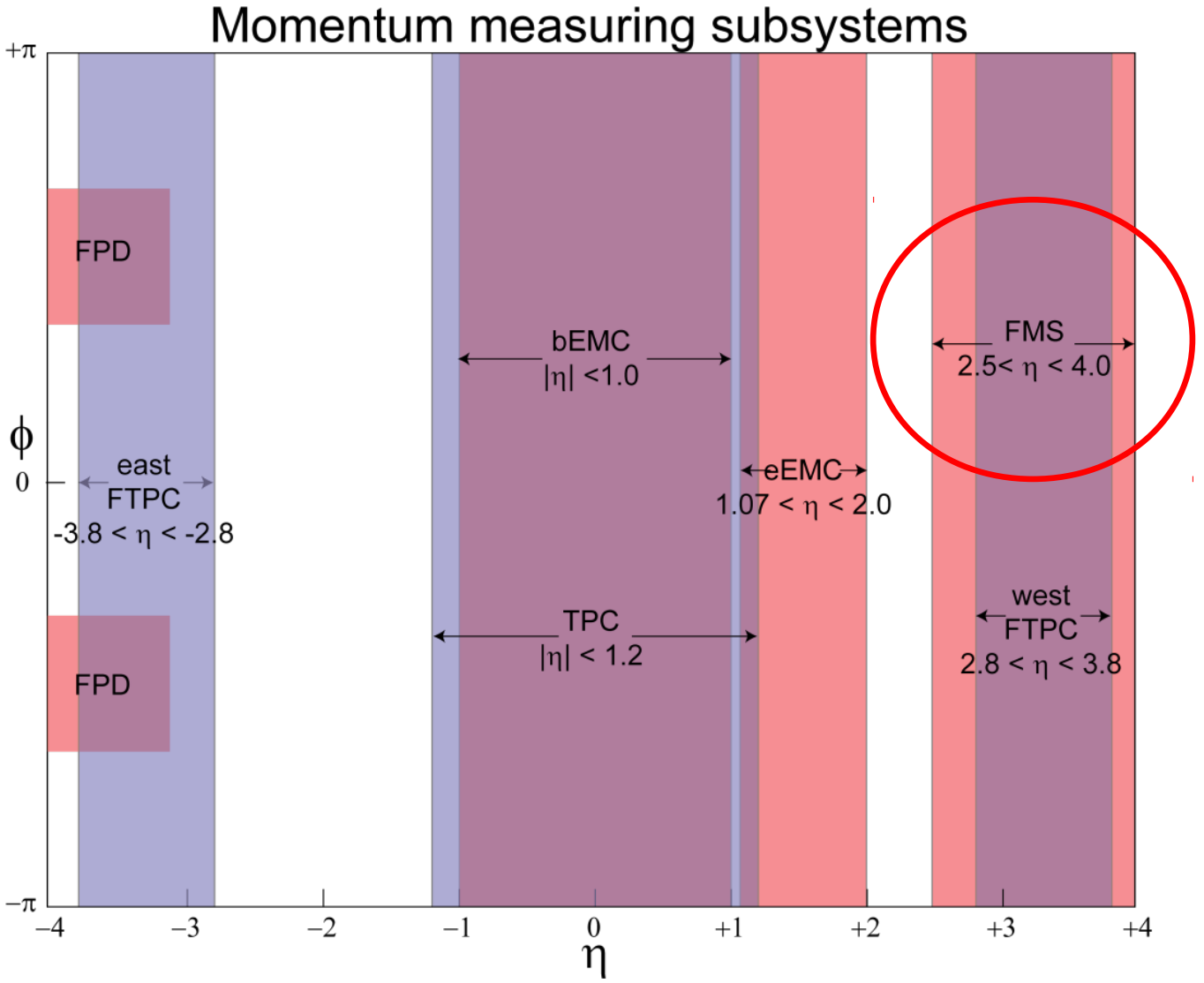

With installation of FMS, STAR EM calorimeter coverage spans most of the pseudo-rapidity region from -1<η<4.

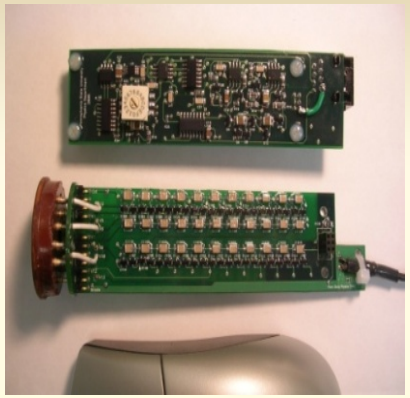

Small Cell PSU Type 224 of 476

Cockcroft-Walton HV bases with computer control through USB. Designed/built in house for FEU-84.

Designed and built at Penn State University

QT board

Readout of 1264 channels of FMS provided by QT boards. Each board has

- **32 analog inputs**
- **5-bit TDC / channel**
- **Five FPGA for data and trigger**
- **Operates at 9.38 MHz and higher harmonics**
- **Produces 32 bits for each RHIC crossing for trigger**
- **12-bit ADC / channel**

Designed and built at UC Berkeley/SSL

Cockroft Walton Voltage Multiplier

Resistor Divider Chain

Simple and cheap to manufacture, but **HV has to be generated somewhere**.
→ External supply of HV → Cable mass

Output impedance (OI) structure does not match the load structure of a PMT.
→ Highest OI at anode, where load is the highest (~mA)
→ Lowest OI at cathode, where load is negligible (~µA)

Due to this mismatch, large quiescent (steady state) current is needed to ensure linearity → **Increased power consumption**

Cockroft-Walton Voltage Multiplier

More complicated, high component count, but **HV is generated on board**
→ No need for external HV cable

Output impedance structure matches a PMT much better → OI is the highest at the top, (cathode) and the lowest at the bottom (anode) of the chain

Operating current is much lower than the resistor divider chain. Furthermore, the chain itself has very low quiescent current → **Reduced power consumption and heat generation**

Full-Wave (Dual Charging Bank) Design

"Full-Wave" CW chain greatly improves the "sagging" and "ripple" in the output voltage caused by the load current. Because these effects strongly depend on the number of stages, it is particularly useful for high stage number CW systems.

- N = Total number of stages
- V_{out} = DC output voltage at the N'th stage
- V_{ripple} = AC ripple voltage at the N'th stage
- f = Frequency of the pulse
- C = Capacitance (constant for all stages)
- I = Load current drawn at the N'th stage

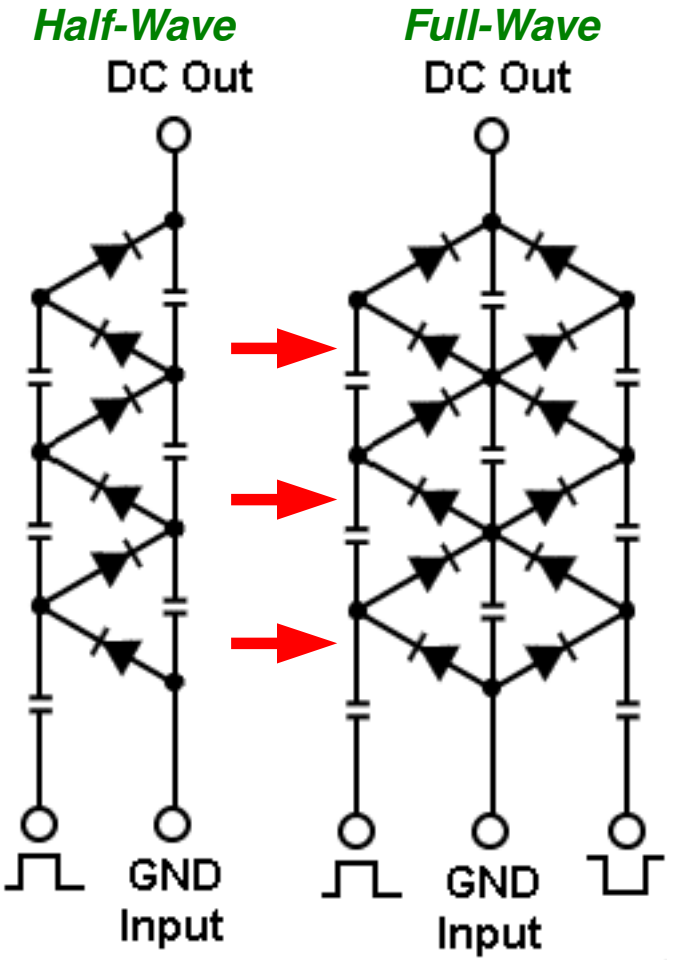

Half-wave CW (Single)

$$V_{ripple} = \frac{IN^2}{fC} \qquad V_{drop} = \frac{I}{fC} \times \left\{ \frac{8N^3 + 3N^2 + N}{6} \right\}$$

Full-wave CW (Dual)

$$V_{ripple} = 0 \qquad V_{drop} = \frac{I}{fC} \times \left\{ \frac{N(N+1)(2N+1)}{6} \right\}$$

Full wave design removes the AC error, and improves the DC error by almost a factor of 4

Feedback-less Design

Commonly, ***CW systems employ a feedback feedback*** to counteract the time varying load and stabilize the output voltage. Output HV is read at the top (cathode), and ***the amplitude and/or frequency of the input is adjusted accordingly.***

- Needs to draw current at the top, ***where output impedance is the highest.***
- Higher precision for the readout leads to higher current draw → ***Feedback can be a major source of voltage drop***
- Feedback can only stabilize the final output. → Even at fixed HV, the relative step size among dynodes varies as a function of load, ***potentially compromising linearity.***
- Slow response of CW chain → ***Difficult to stabilize the feedback circuit***

Full-Wave CW Provides Excellent Stability → No Need for Feedback

- ***Make the chain robust by itself, instead of letting it sag and then fixing it.***
- ***22-stage CW*** with V_{min} ~ 1200V and V_{max} ~ 1800V
- ***No measurable ripple***
- ***V_{dqp} ~ 1% of the output voltage → High stability for step size***
- Improved linearity over the resistive divider base it replaces
- Less than 1 pC pedestal for 60nS gate
- Output voltage readout with ~1μA current draw → Low resolution, for monitoring only

I^2C Serial Bus

1. ***I^2C is a low speed (~100kbits/sec) two line serial bus*** developed by Philips for use in consumer electronics, such as TV and computer peripherals.

2. Due to its wide usage and the lack of licensing fee, ***parts compatible with I^2C are abundant and cheap.***

3. It's ***flexible, easy to use, and relatively power efficient.***

On-board Intelligence via I^2C Bus

We use I^2C to control and read out the HV remotely. ***The HV set point can be stored on each base, which becomes a start-up value.*** HV read out is used for diagnostic.

- 8-bit Digital Potentiometer with EEPROM → Non-volatile HV control
- 8-bit 4 channel ADC → HV read back, voltage regulation diagnostics

There are only two supply voltages needed to operate the device. (+9V, +30V) Along with I^2C, we have ***total of four low-voltage, low-power input lines and no analog signal.***
→ No need for fancy cables!

- Operating power consumption ***~200mW***
- ***Cat5e cable and connector*** →Polarized, locking, reliable, and low cost

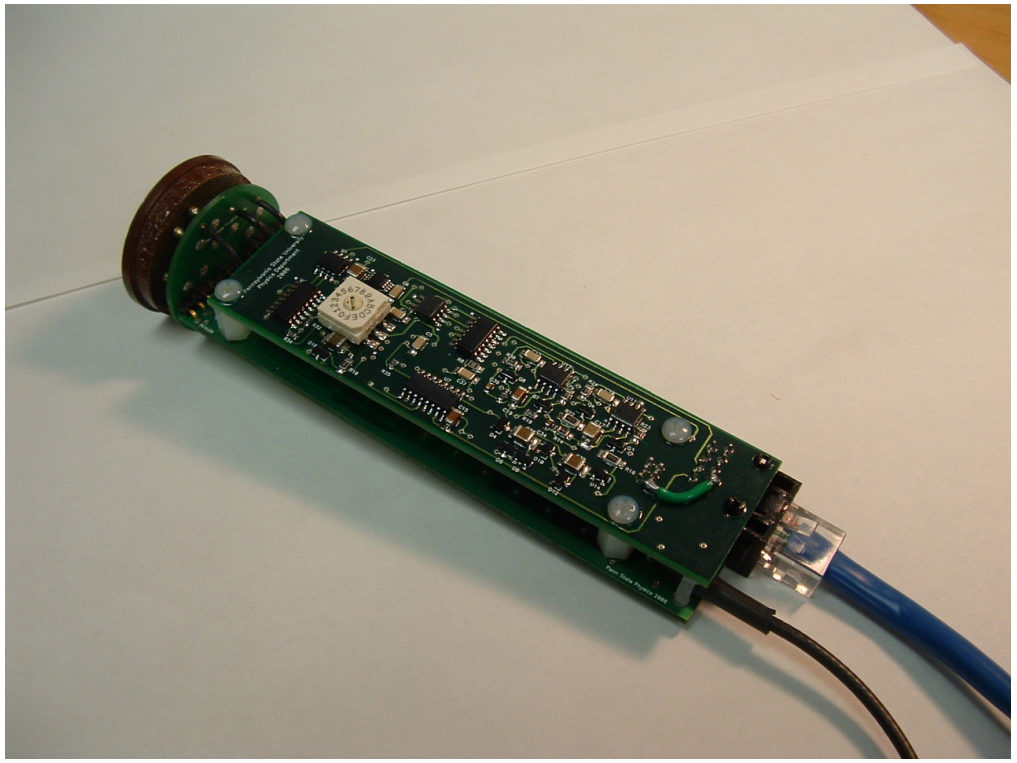

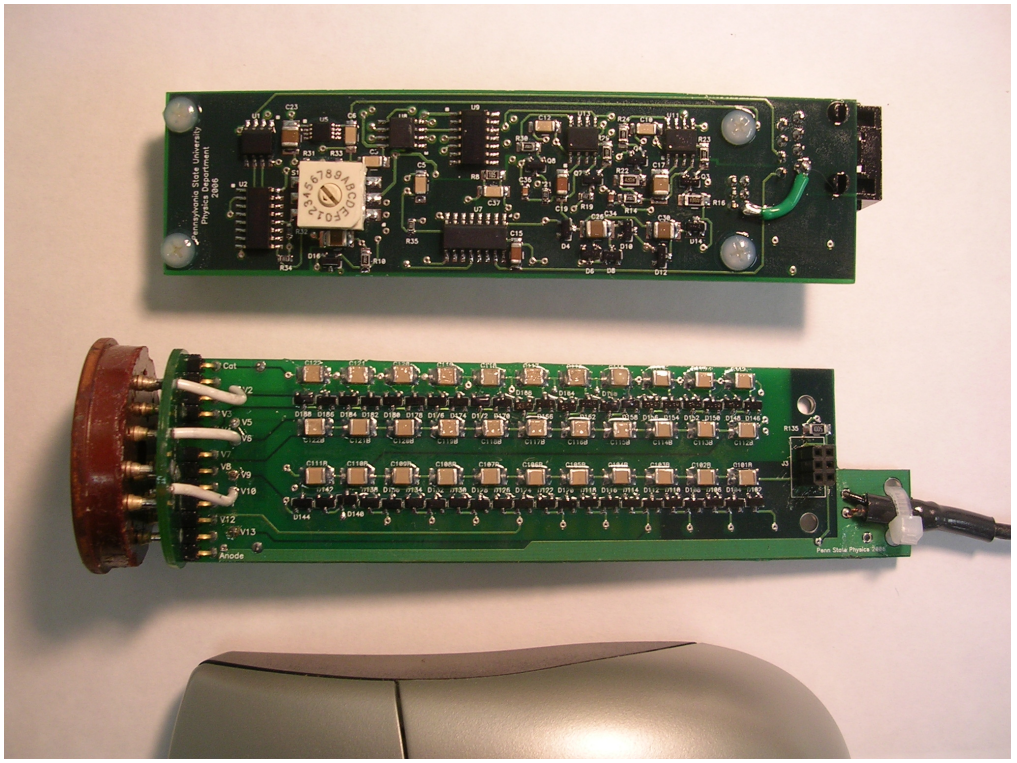

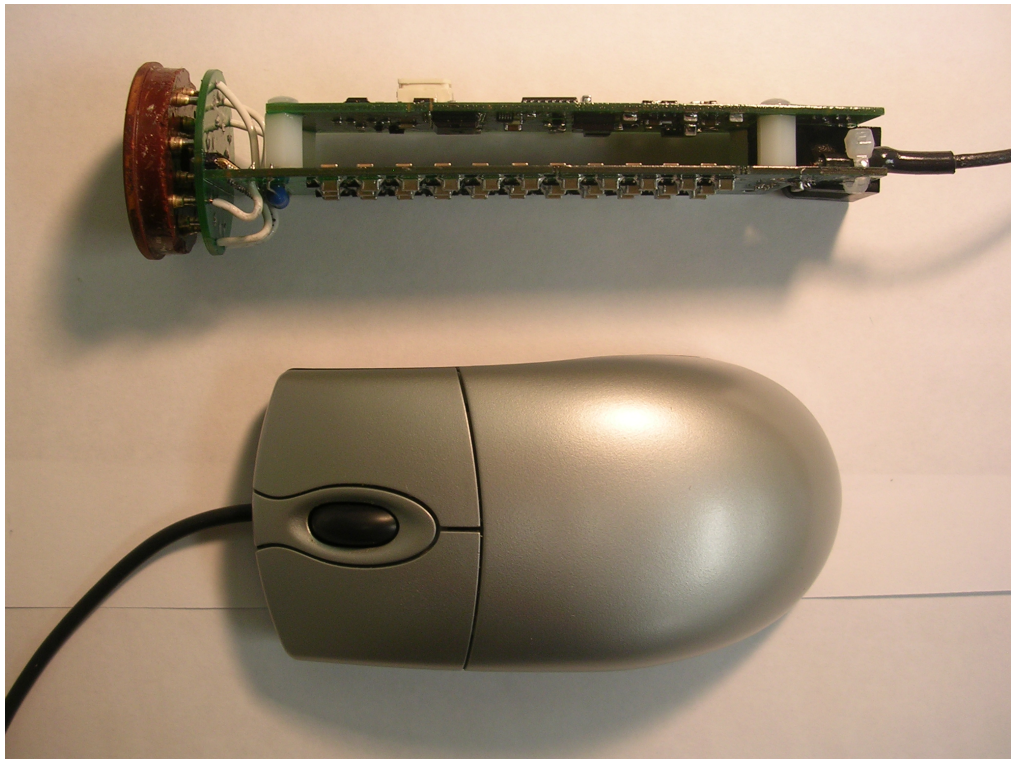

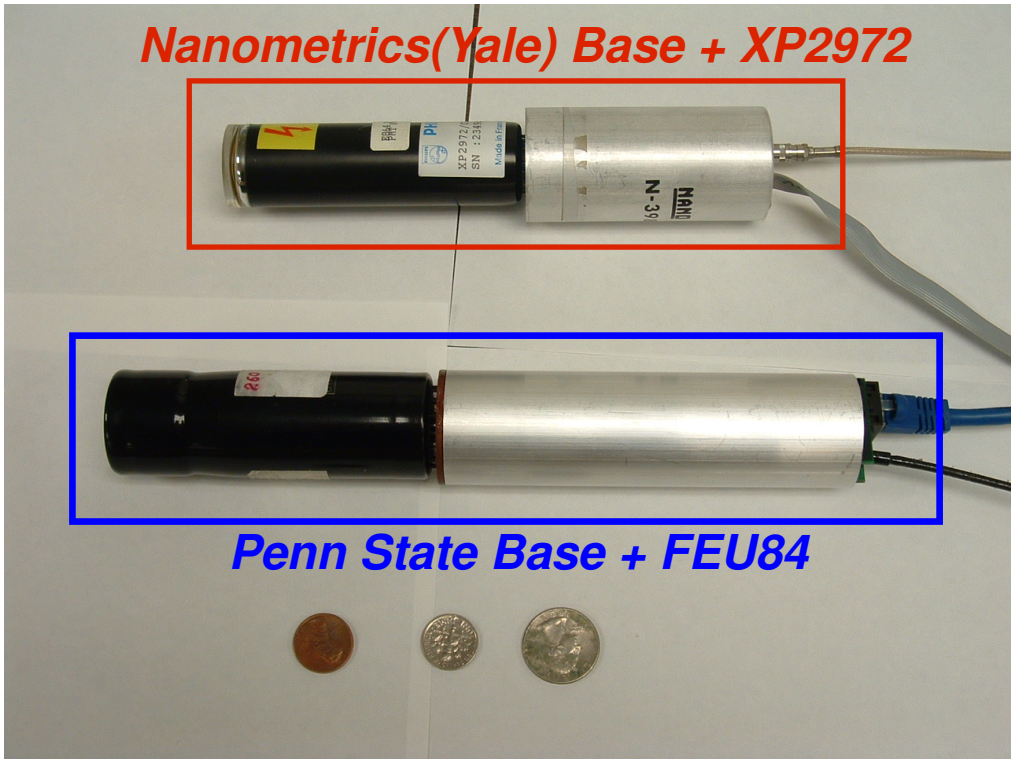
Nanometrics(Yale) Base + XP2972
Penn State Base + FEU84

Nanometrics(Yale) Base – Interfacing Two systems

1. ***Cockroft-Walton type bases*** made by Nanometric for **AGS E864**, and donated to the FMS project by the good folks at Yale University

2. ***No on-board intelligence*** → Requires two analog lines to set and monitor the high voltage. → ***Need for external controller***

3. Similar power consumption to Penn State bases. (~200mW)

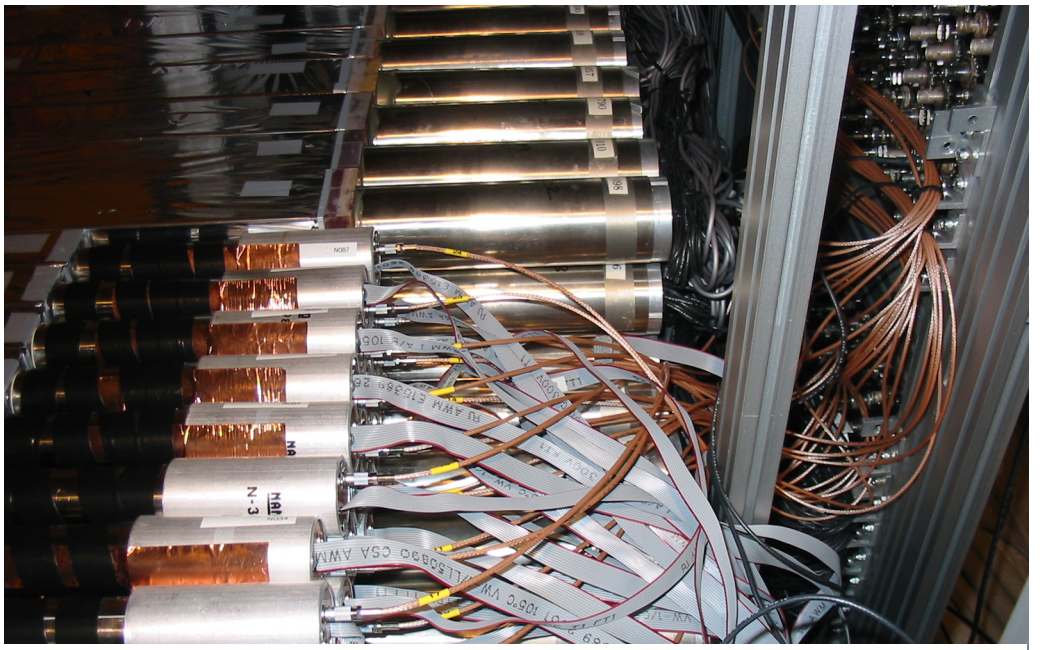

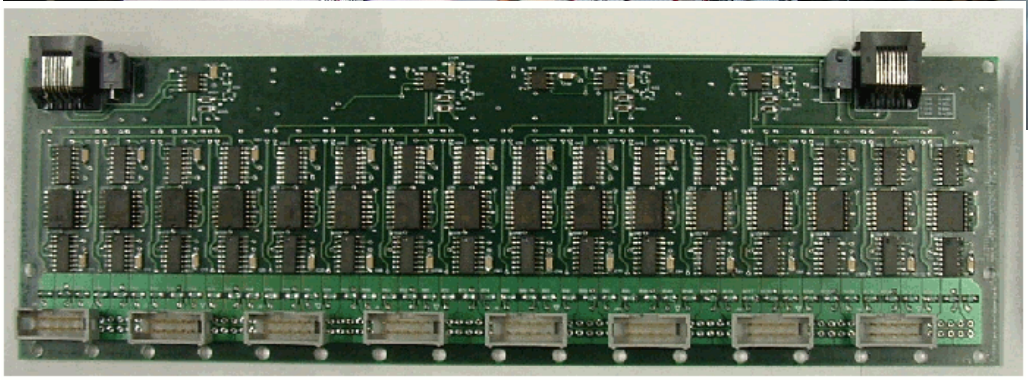

"Yale Controller"

→ ***I²C front end/voltage distribution similar to the Penn State bases'***

1. Uses the same Cat5e connector to receive "Penn State" type voltages and I2C signal.

2. Converts the voltages and generates/reads the analog signals to control 16 Yale bases.

3. ***Allows virtually transparent higher level control of Penn State and Yale type bases.***

Master Controller

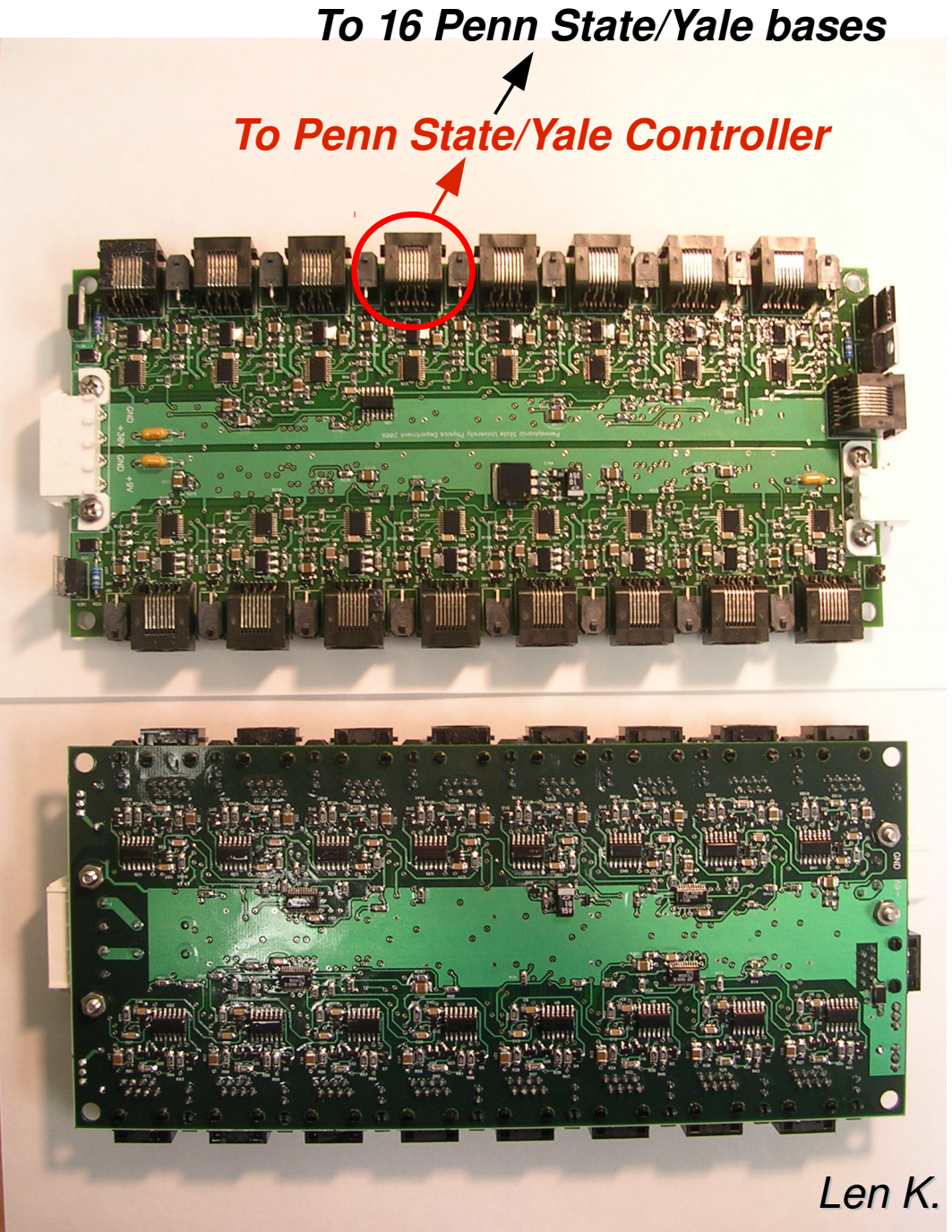

At the top of the control sits the "***Master Controller***," which is ***run through USB by a Windows PC*** via off the shelf USB to I^2C converter.

- Controls up to ***256 phototube bases by connecting to any combination of 16 Penn State/Yale controller***

- Distribute three DC voltages (+9V, +30V, -6V) to 16 PSU/Yale controllers through computer controlled transistor switches

- Provide ***over-current and over-voltage protection*** for the three voltages

- Provide ***I^2C serial bus multiplexing for channel by channel HV control***

- ***Sequential turn-on*** feature reduces transient current load on power supplies

Len K. Eun

FMS Small Cells HV System Overview

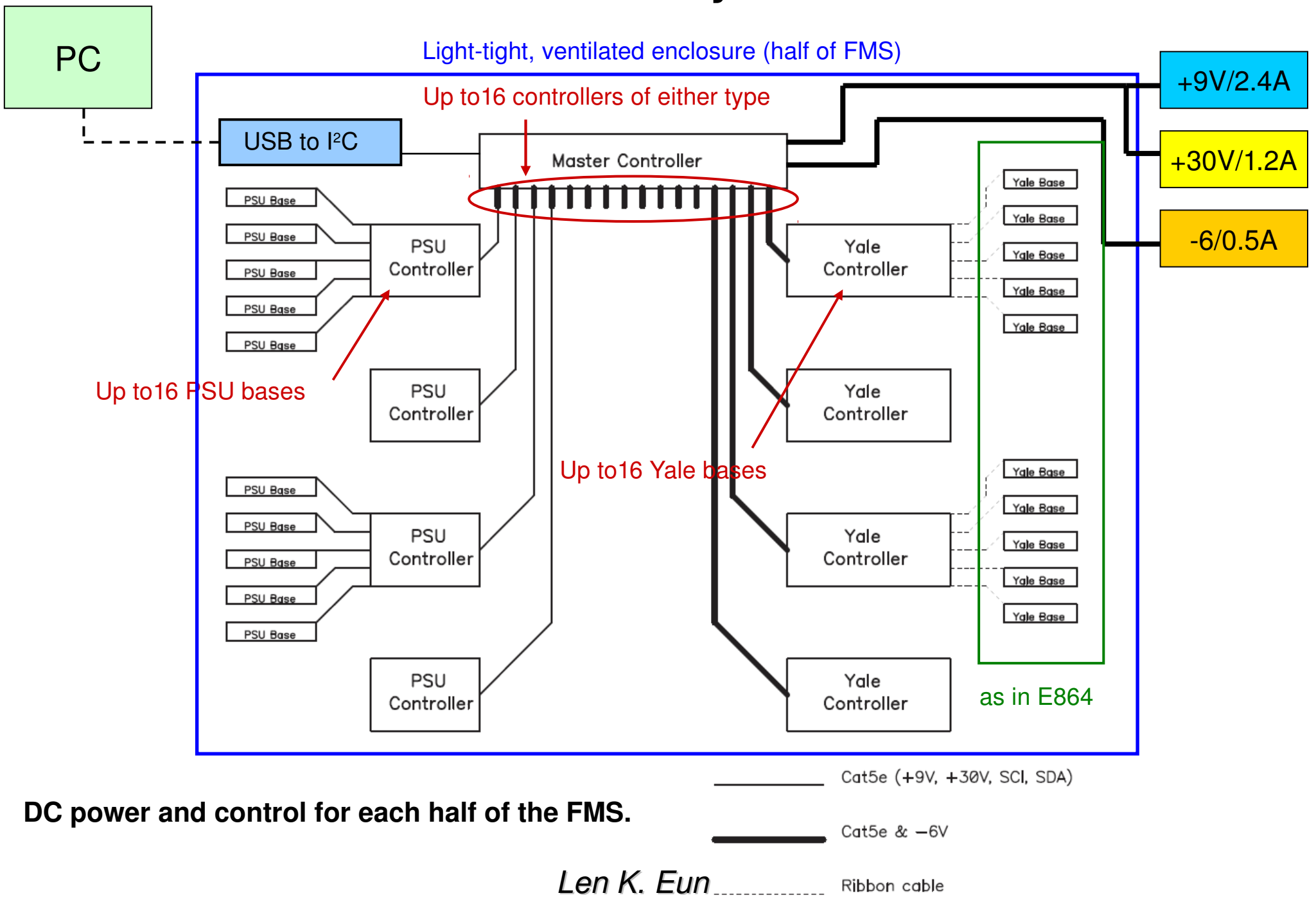

DC power and control for each half of the FMS.

Len K. Eun

SUMMARY

1. The STAR Forward Pion Detectors (FPD) at RHIC measured cross-section for π^0 meson in $<\eta>$=3.3~4.0 region during $\sqrt{s}$=200GeV p+p collision. It was found to be consistent with pQCD calculations.

2. From RHIC run3 to run8, the FPD measured large forward single spin asymmetry, A_N, for π^0. The x_F dependence of A_N was qualitatively consistent with theoretical predictions. p_T dependence, however, differed significantly from predictions based on all currently existing models

3. In addition to π^0, η mesons were observed in the east FPD during RHIC run6. We measured the single spin asymmetry in the π^0 and the η mass regions, at $<\eta>$~3.65 and x_F above 0.4. **We found the A_N in η mass region to be ~4 standard deviation greater than the A_N in π^0 mass region from 55GeV to 75GeV. (x_F=0.55~0.75)**

4. Based on the same RHIC run6 east FPD data set used for the η asymmetry measurement, **we now have the preliminary result for the cross-section ratio between π^0 and η for x_F>0.45. While systematics are relatively large, the result is consistent with the expected origin of the observed π^0's and η's from jet fragmentation.**

5. For the cross-section measurement, energy scale uncertainty remains the primary systematics. The culprit here is the shower shape discrepancy between the data and Geant 4, which limits the absolute energy scale uncertainty to no better than 4~5%. We are currently working on this issue, and **we aim to measure the absolute cross-section for both π^0 and η for x_F>0.45 in the near future.**

THE END